

OPEN ACCESS

# Significant Improvements to Si Calendar Lifetime Using Rapid Electrolyte Screening via Potentiostatic Holds

To cite this article: Ankit Verma *et al* 2024 *J. Electrochem. Soc.* **171** 070539

View the [article online](#) for updates and enhancements.

## You may also like

- [Reversible Self-discharge of LFP/Graphite and NMC811/Graphite Cells Originating from Redox Shuttle Generation](#)  
Sebastian Buechele, Eric Logan, Thomas Boulanger *et al.*
- [Carbon Corrosion in PEM Fuel Cells and the Development of Accelerated Stress Tests](#)  
Natalia Macauley, Dennis D. Papadias, Joseph Fairweather *et al.*
- [Effect of Catalyst and Catalyst Layer Composition on Catalyst Support Durability](#)  
Siddharth Komini Babu, Rangachary Mukundan, Chunmei Wang *et al.*

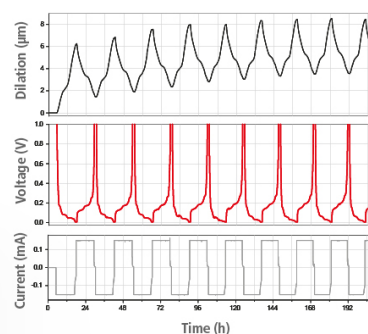
## Watch Your Electrodes Breathe!

Measure the Electrode Expansion in the Nanometer Range with the ECD-4-nano.

- ✓ Battery Test Cell for Dilatometric Analysis (Expansion of Electrodes)
- ✓ Capacitive Displacement Sensor (Range 250  $\mu\text{m}$ , Resolution  $\leq 5$  nm)
- ✓ Detect Thickness Changes of the Individual Half Cell or the Full Cell
- ✓ Additional Gas Pressure (0 to 3 bar) and Temperature Sensor (-20 to 80° C)



**EL-CELL**<sup>®</sup>  
electrochemical test equipment



See Sample Test Results:



Download the Data Sheet (PDF):



Or contact us directly:

+49 40 79012-734

[sales@el-cell.com](mailto:sales@el-cell.com)

[www.el-cell.com](http://www.el-cell.com)



# Significant Improvements to Si Calendar Lifetime Using Rapid Electrolyte Screening via Potentiostatic Holds

Ankit Verma,<sup>1,z</sup> Maxwell C. Schulze,<sup>1</sup> Andrew Colclasure,<sup>1</sup> Marco-Tulio Fonseca Rodrigues,<sup>2</sup> Stephen E. Trask,<sup>2</sup> Krzysztof Puppek,<sup>3</sup> and Daniel P. Abraham<sup>2,z</sup>

<sup>1</sup>Energy Conversion and Storage Systems Center, National Renewable Energy Laboratory, Golden, Colorado, United States of America

<sup>2</sup>Chemical Sciences and Engineering Division, Argonne National Laboratory, Argonne, Illinois 60439, United States of America

<sup>3</sup>Applied Materials Division, Argonne National Laboratory, Argonne, Illinois 60439, United States of America

Silicon-based lithium-ion batteries exhibit severe time-based degradation resulting in poor calendar lives. This has been identified as the major impediment towards commercialization with cycle life considered a solved issue through nanosizing and protective coatings allowing over 1000 cycles of life to be achieved. In this work, rapid screening of sixteen electrolytes for calendar life extension of Si-rich systems (70 wt% Si) is performed using the voltage hold (V-hold) protocol. V-hold significantly shortens the testing duration over the traditional open circuit voltage reference performance test allowing us to screen electrolytes within a span of two months. We find a novel ethylene carbonate (EC) free electrolyte formulation containing lithium hexafluorophosphate (LiPF<sub>6</sub>) salt, and binary solvent mix of fluoroethylene carbonate (FEC), ethyl methyl carbonate (EMC) that extends calendar life of Si cells as compared to conventional EC based electrolyte. Our coupled experimental-theoretical analysis framework provides a decoupling of the parasitic currents during V-hold, allowing us to extrapolate the capacity loss to predict semiquantitative calendar lifetimes. Subsequently, cycle aging and oxidative stability tests of the EC free system also show enhanced performance over baseline electrolyte.

© 2024 The Author(s). Published on behalf of The Electrochemical Society by IOP Publishing Limited. This is an open access article distributed under the terms of the Creative Commons Attribution 4.0 License (CC BY, <http://creativecommons.org/licenses/by/4.0/>), which permits unrestricted reuse of the work in any medium, provided the original work is properly cited. [DOI: 10.1149/1945-7111/ad6376]



Manuscript submitted April 8, 2024; revised manuscript received June 19, 2024. Published July 25, 2024.

Supplementary material for this article is available [online](#)

Current lithium-ion batteries (LIBs) have reached energy densities of  $\geq 270 \text{ Wh kg}^{-1}$ ,  $650 \text{ Wh L}^{-1}$  using predominantly graphite-based anodes.<sup>1</sup> Commercial cell manufacturers have started using graphite-silicon (Gr-Si) blends and steadily increased the weight proportion of Si in the blended anode to 5% to enhance the energy density while maintaining good cycle and calendar life.<sup>2–4</sup> Next generation LIBs could reach energy density metrics of  $\geq 350 \text{ Wh kg}^{-1}$ ,  $750 \text{ Wh L}^{-1}$  by incorporating silicon dominant anodes.<sup>5</sup> Several industry leaders are using 100% Si anodes (no graphite) with nanowire silicon technology promising energy densities as high as  $450 \text{ Wh kg}^{-1}$ ,  $1200 \text{ Wh L}^{-1}$ .<sup>6–8</sup>

In the last two decades, cycling of 100% Si anodes was identified as the major challenge due to its  $\sim 300\%$  volume change at the particle level with full lithiation/delithiation.<sup>9</sup> This arises from the high molar volume of Li in Si host ( $9 \text{ cm}^3/\text{mol}$ ) as compared to Gr host ( $1.14 \text{ cm}^3/\text{mol}$ ) combined with large uptake of Li in Si host (up to 4.4 Li per Si atom) as compared to Gr host (up to 1 Li per 6 C atoms).<sup>10–12</sup> Consequently, the Si particle and the solid electrolyte interphase fractures upon cycling resulting in repeated loss of lithium inventory (LLI) and active material (LAM) in each cycle.<sup>13,14</sup> LLI occurs due to solvent reduction leading to lithium incorporation into the solid electrolyte interphase and this lithium is no longer available for intercalation. LAM occurs due the Si particle fracturing and becoming electronically isolated such that part of the Si is no longer available for lithiation.<sup>15,16</sup> Several strategies to mitigate the cycle life issue have been explored including nanosized Si particles,<sup>17–19</sup> buffer layers on Si core,<sup>20,21</sup> electrolyte additives<sup>22–24</sup> to form non rupturing elastomeric solid electrolyte interphase. These have successfully increased the Si cycle life to up graphite levels (500–1000 cycles before 20% capacity fade).<sup>25</sup> It is interesting to note that typically cycle life tests are run at C/3, so the average test time to perform 1000 cycles is 6000 h (=250 d/ $\sim 8$  months).

In 2021, McBrayer et al. identified calendar life as the major problematic issue for Si containing LIBs.<sup>25</sup> The US Department of Energy (DOE) collected information on Si cells from leading industrial manufacturers and they exhibited 500–1000 cycles with  $>300 \text{ Wh kg}^{-1}$  energy densities. However, calendar lives of the same cells plateaued at an upper limit of 20 months ( $<2$  years) at high state of charge. This represents a wide gap from the 10-year calendar life metric that is needed for commercial application. Calendar life test activates time-based degradation (instead of energy throughput-based degradation) leading to loss of lithium inventory.<sup>26–28</sup> This temporal degradation mode is shrouded in cycle life tests as the average cycle life test only lasts 8 months. Cycle life test also swings the cell's state of charge (SOC) from 0 to 100%, while the calendar life test typically maintains the cell at a constant SOC. Higher degradation is generally observed near full state of charge because of greater propensity for solid electrolyte interphase formation.<sup>29</sup> Chemical contributions to silicon calendar aging (e.g. SEI formation, dissolution) can dominate over mechanical contributions (e.g. volume expansion, fracture).<sup>30</sup> It is interesting to note that SEI on silicon anodes can be uniquely non-passivating, exhibiting breathing characteristics from deposition-dissolution dynamics.<sup>31</sup>

Traditional calendar life test protocols consist of repeated capacity/power density checks after month long rests (open circuit voltage reference performance test, OCV RPT) to see how the cells are degrading.<sup>32,33</sup> This requires extensive testing to get enough datapoints for regression fits that can be extrapolated towards a quantitative calendar life.<sup>34–36</sup> For graphite, it is well established that  $\sim 1$ – $2$  years of testing can be used with empirical models to project lifetimes out to an order of magnitude higher duration (10–20 years) relatively well.<sup>37,38</sup> We don't know how much testing time is needed for silicon currently. Also, OCV RPT is a slow test, good for quantitative lifetime estimates but unwieldy for fast material development that can improve calendar life. Rapid screening requires an electrochemical protocol that can answer the question: which Si anode material, electrolyte formulation, out of multiple candidates, is better for calendar life in a short testing timeframe? Potentiostatic hold (or voltage hold) protocol possesses the attributes


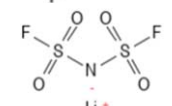
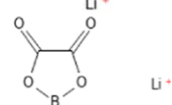
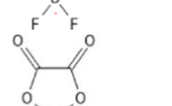
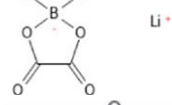
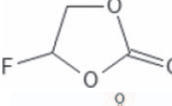
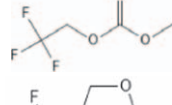
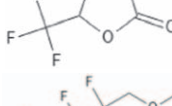
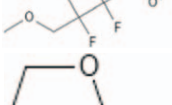
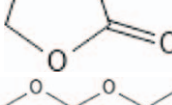
<sup>z</sup>E-mail: [ankit.verma@nrel.gov](mailto:ankit.verma@nrel.gov); [abraham@anl.gov](mailto:abraham@anl.gov)

to answer this question and has been chosen as the calendar life testing vehicle for this work.<sup>39</sup> Schulze et al. discussed the V-hold protocol for Gr, Si cells pairing the anode with a flat potential cathode like lithium iron phosphate (LFP) to maintain a constant anode potential during the hold.<sup>40</sup> This work standardized the V-hold protocol providing a knowhow of qualitative calendar lifetime screening that can answer if one electrolyte is better than the other. Verma et al. used three-electrode cells to understand the evolution of anode, cathode potentials during the V-hold with two electrolyte systems: fluorine free LiBOB electrolyte and fluorine rich LiPF<sub>6</sub> electrolyte.<sup>41</sup> This enabled a deeper understanding of the simultaneous physical processes occurring during the V-hold: reversible cathode delithiation to supply Li<sup>+</sup> ions into the electrolyte, reversible anode lithiation from these Li<sup>+</sup> ions reaching anode and intercalating, parasitic SEI formation from reduction of the electrolyte at the anode, and parasitic anode delithiation from anode host Li further reducing solvents to form the SEI. Finally, this resulted in an analysis framework to quantify the reversible and irreversible proportion of the capacity exchanged during the hold and correlate it to semiquantitative calendar life. In literature, long OCV rests up

to 500 h have also been explored to estimate the total storage loss and its deconvolution into irreversible SEI loss and reversible self-discharge loss for multiple electrolytes.<sup>42,43</sup> Long potentiostatic holds and OCV rests are complementary techniques to rapidly evaluate calendar life stability of electrolytes. V-hold provides a more detailed time-resolved capacity, current dataset for capacity loss predictions. In comparison, OCV rests provides the following datapoints: capacity before rest, voltage decay during rest, capacity after rest and capacity from the reference performance test cycle to compute the irreversible loss.

In this work, we use the V-hold protocol on Si/LFP cells with sixteen different electrolyte formulations to identify new EC free electrolytes that have better calendar life than the conventional EC based formulations. These electrolyte formulations have previously been used in lithium-ion battery literature with graphite/silicon/lithium metal anodes for cycle life improvements.<sup>44–49</sup> Prior literature on silicon anodes shows EC can be a bad actor for silicon anodes with FEC and vinylene carbonate (VC) as proposed additives for good SEI stability.<sup>50</sup> FEC is particularly well explored with salient results highlighted below:

**Table I. List of salts and solvents used in this study. Chemical structure created using PubChemSketcher V2.4 (<https://pubchem.ncbi.nlm.nih.gov/edit3/index.html>).**

Compounds	Full chemical name	Abbreviated name	Chemical formula	Structure	References
Fluorinated salts	lithium hexafluorophosphate	LiPF <sub>6</sub>	LiPF <sub>6</sub>		69, 70
	lithium bis(fluorosulfonyl)imide	LiFSI	LiF <sub>2</sub> NO <sub>4</sub> S <sub>2</sub>		71, 72
	lithium difluoro(oxalato)borate	LiDFOB	LiBF <sub>2</sub> C <sub>2</sub> O <sub>4</sub>		73
Non-fluorinated salt	lithium bis(oxalato)borate	LiBOB	LiB(C <sub>2</sub> O <sub>4</sub> ) <sub>2</sub>		49, 74
Fluorinated solvents	fluoro ethylene carbonate	FEC	C <sub>3</sub> H <sub>3</sub> FO <sub>3</sub>		52, 75
	methyl (2,2,2-trifluoroethyl) carbonate	FEMC	C <sub>4</sub> H <sub>5</sub> F <sub>3</sub> O <sub>3</sub>		76, 77
	trifluoropropylene carbonate	TFPC	C <sub>4</sub> H <sub>3</sub> F <sub>3</sub> O <sub>3</sub>		78
	1,4-dimethoxy-2,2,3,3-tetrafluorobutane	FDMB	C <sub>6</sub> H <sub>10</sub> F <sub>4</sub> O <sub>2</sub>		79, 80
Non-fluorinated solvents	ethylene carbonate	EC	C <sub>3</sub> H <sub>4</sub> O <sub>3</sub>		69, 81
	ethyl methyl carbonate	EMC	C <sub>4</sub> H <sub>8</sub> O <sub>3</sub>		69, 81

- (1) Thinner and more uniform SEI with FEC as compared to without FEC.<sup>22,51–53</sup>
- (2) Electronically insulating LiF species incorporated in the SEI with FEC.<sup>51,54–57</sup>
- (3) Crosslinked polymer species providing mechanical compliance incorporated in the SEI with FEC.<sup>31,50,52,53,58–62</sup>
- (4) LEDC formed from EC decomposition has lower stability on the surface of silicon particles than on graphite during electrochemical cycling.<sup>46,63,64</sup>
- (5) Lower Li-trapping inside Si anodes happens with FEC.<sup>65</sup>

With respect to calendar life, Malkowski et al.<sup>46</sup> have performed 180 h voltage holds on 80 wt% Paraclete Silicon and show that EC and LiPF<sub>6</sub> decomposition lead to higher hold currents and poorer passivation, while EMC does not play a role.

The rest of the article is divided as follows. Details of the experimental methods including materials, cell design and electrochemical testing protocol are elaborated first. The theoretical foundations of V-hold calendar lifetime analysis framework to deconvolute reversible and irreversible capacities is summarized next. Subsequently, we perform this analysis on Si/LFP cells with sixteen different electrolytes divided into four different groups to compare calendar life performance. Finally, cycle life and oxidative stability analysis on our best performing novel electrolyte system is performed using Si/NMC cells to understand impacts to cycle life. Additional data to support our analysis are presented in the Supporting Information (SI) which is referenced in the text with the designator “S”.

### Experiments: Materials, Cell Design and Electrochemical Testing

The positive and negative electrode sheets were fabricated at the Cell Analysis, Modeling and Prototyping (CAMP) facility at Argonne National Laboratory. Table I lists the chemical name, chemical formula and structure of salts and solvents used in this study; Table II lists the sixteen electrolyte formulations used in this study. The electrolytes are chosen to represent a mix of baseline formulations and novel formulations that are common in literature to stabilize graphite, silicon and lithium metal anodes.<sup>44,45,66–68</sup> Electrolytes were prepared in-house at Argonne’s Materials Engineering Research Facility (MERF). EC, EMC were purchased from BASF and FEC from Solvay. FEMC, TFPC, FDMB were synthesized in house in MERF. LiPF<sub>6</sub> salt was obtained from Strem Chemicals. LiBOB and LiDFOB salts were synthesized in MERF. LiFSI salt was purchased from Arkema. The commercial solvents and salts were battery grade (moisture <20 ppm) and were used as

received. In-house solvents and salts were also maintained below the same moisture level. Electrolytes were made in a glovebox (<1 ppm O<sub>2</sub>, H<sub>2</sub>O). Solvents were pre-mixed in the corresponding weight ratios as outlined in Table I, for example, for Gen2 and baseline Gen2F3 electrolyte EC, EMC were premixed in 30/70 w/w% ratio. Then, LiPF<sub>6</sub> salt was added to the solvent mixture, the mixture was stirred and filtered to accurate volumes to obtain the 1.2 M salt concentration. Then, an appropriate amount of FEC was added to get the baseline electrolyte. Similar steps were followed to prepare the remaining electrolyte systems.

For calendar life evaluation using voltage holds, Si/LFP coin cells are built. The anode has 70 wt% Paraclete nSi/C, 150 nm Si (carbon-coated Si), 15 wt% C45 carbon conductive additive for enhanced electron transport and 15 wt% lithiated polyacrylic acid (LiPAA) binder. Cathode is 90 wt% Johnson Matthey LiFePO<sub>4</sub>, 5 wt% Timcal C45 carbon, 5 wt% Solvay 5130 PVDF Binder. Cycle life evaluation is performed using Si/NMC811 coin cells. Anode is the same as calendar life tests while the cathode has 90 wt% NMC811, 5 wt% Timcal C45 carbon and 5 wt% Solvay 5130 PVDF Binder. Tables S1 and S2 show the electrode specifications for the calendar life and cycle life tests.

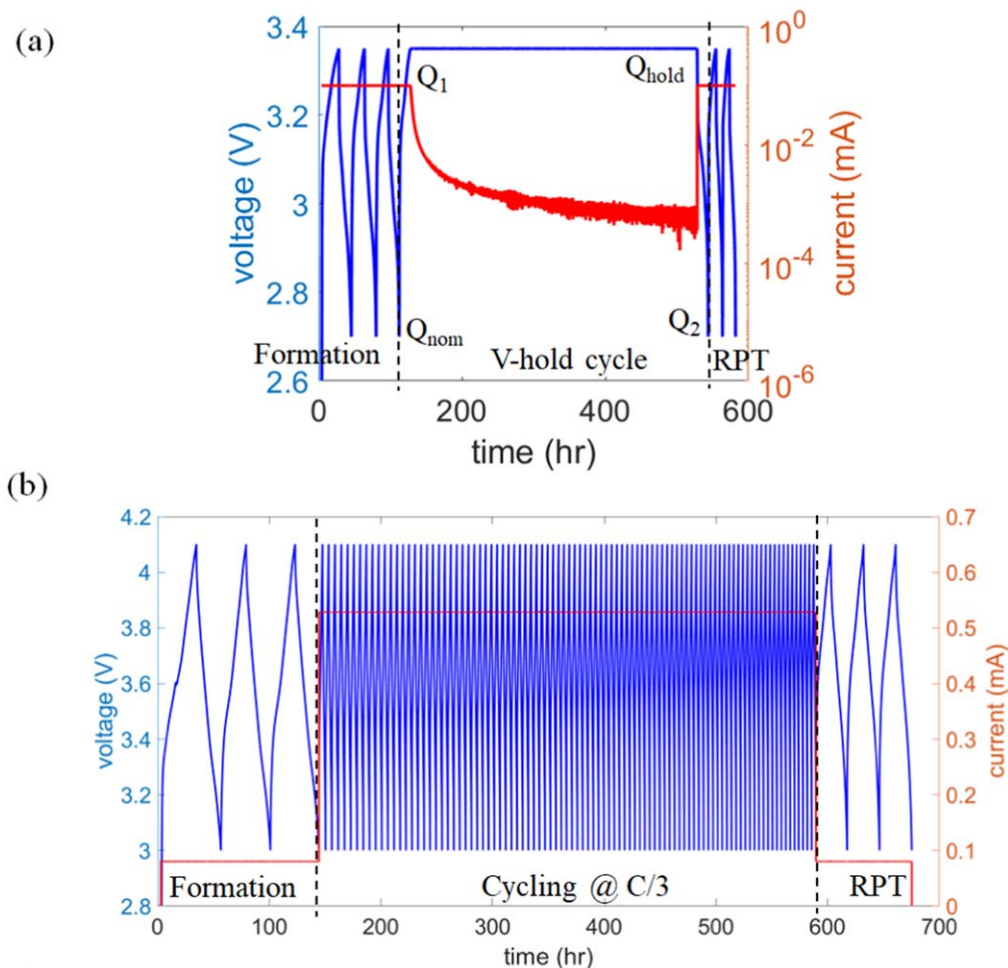
Electrochemical cells comprising a Si anode, LFP (calendar aging)/NMC811 (cycle aging) cathode and electrolytes were assembled under argon (Ar) atmosphere in a glovebox. Each cell contained a 14 mm diameter cathode punch paired with a 15 mm diameter anode punch separated by a Celgard 2500 separator. Electrochemical calendar and cycle life testing of the cells was performed using a Maccor Series 4000 test unit at 30 °C. Calendar life was evaluated using the V-hold protocol consisting of a three constant current (CC) formation cycles at C/20 rate followed by a constant current constant voltage (CCCV) hold cycle and ends with two additional diagnostic CC cycles at C/20 rate resulting in a total of six cycles. During calendar life test with Si/LFP, the cell voltage varies between 2.7 V and 3.35 V. The 4th cycle is the V-hold cycle consisting of a C/20 charge up to 3.35 V followed by a 400 h V-hold at the top of charge and subsequent discharge to 2.7 V. Figure 1a shows a standard V-hold calendar life protocol consisting of the formation, V-hold and RPT cycles. Since the calendar life protocol uses slow RPTs, we don’t expect any electrolyte rate limitations to affect the analysis. Cycle life is evaluated using Si/NMC cells with 3 slow C/20 formation cycles followed by 94 C/3 cycles and subsequently ending with diagnostic 3 slow C/20 cycles and tracking the capacities in each cycle. The voltage window for cycle aging is 3–4.1 V. Figure 1b shows a standard cycling protocol. Triplicates were tested for each condition and representative data is shown.

We chose the Si-LFP cell configuration for calendar life to ensure that the Si potentials reached during the V-hold as well as in all

**Table II. List of electrolytes used in this study.**

S. No.	Electrolyte	Is EC present?	Is F present?
1.	Gen2: 1.2 M LiPF <sub>6</sub> in EC:EMC (3:7 w/w)	✓	✓
2.	Gen2F3: 1.2 M LiPF <sub>6</sub> in EC:EMC (3:7 w/w) + 3 wt.% FEC (baseline)	✓	✓
3.	0.7 M LiBOB in EC:EMC (3:7 w/w)	✓	×
4.	1.2 M LiDFOB in EC:EMC (3:7 w/w)	✓	✓
5.	1.5 M LiPF <sub>6</sub> in FEC:EMC (1:9 w/w)	×	✓
6.	1.4 M LiPF <sub>6</sub> + 0.1 M LiBOB in FEC:EMC (1:9 w/w)	×	✓
7.	1.4 M LiPF <sub>6</sub> + 0.1 M LiDFOB in FEC:EMC (1:9 w/w)	×	✓
8.	1.4 M LiPF <sub>6</sub> in FEC:EMC (1:9 w/w)	×	✓
9.	1.8 M LiPF <sub>6</sub> in FEC:EMC (1:9 w/w)	×	✓
10.	1.5 M LiPF <sub>6</sub> in FEC:FEMC (1:9 w/w)	×	✓
11.	1.2 M LiPF <sub>6</sub> in FEC:FEMC (1:9 w/w)	×	✓
12.	1.5 M LiPF <sub>6</sub> in FEC:TFPC (1:9 w/w)	×	✓
13.	1.5 M LiPF <sub>6</sub> in FEC:TFPC: FEMC (1:2:7 w/w)	×	✓
14.	1.2 M LiFSI in FEC:FEMC (1:9 w/w)	×	✓
15.	1 M LiFSI in FDMB	×	✓
16.	0.8 M LiFSI + 0.2 M LiPF <sub>6</sub> in FDMB	×	✓





**Figure 1.** Standard experimental electrochemical protocol for (a) calendar and (b) cycle life evaluation with Si-LFP and Si-NMC coin cells respectively.

cycles are the same across all electrolytes tested. This is enabled by the flat potential profile of LFP electrodes and the excess Li inventory in our V-hold tests with N:P ratio 1:3. Our estimated Si anode capacity is 1 mAh/cm<sup>2</sup> and 3.06 mAh/cm<sup>2</sup> for LFP cathode. During the V-hold, the cell potential is at 3.35 V. In a half cell, the LFP charge plateau is at 3.46 V while the discharge plateau is around 3.40 V.<sup>82</sup> So, the LFP is always at a constant potential during the V-hold if the entire Li inventory is not exhausted and LFP does not reach full delithiation/lithiation. The silicon stays at a constant potential of ~110 mV for 400 h. At 400 h of constant voltage charge, we expect the silicon to reach similar lithiation state across all electrolytes. Also, total Li loss during the voltage hold experiment calculated by summing up the cumulative irreversible loss in each cycle lies in the range of 0.86–1.53 mAh/cm<sup>2</sup> for the best to worst performing electrolytes which is significantly less than the 3 mAh/cm<sup>2</sup> Li present in the LFP cathode. So, the LFP will stay in its flat potential profile and Si will always reach the same potential across all electrolytes tested.

### Deconvolution of Hold Capacity into Reversible and Irreversible Capacity

The estimation of the irreversible capacity loss is described in detail in an earlier work.<sup>41</sup> Here, we present a concise version. Let  $Q_{nom}$ ,  $Q_1$ ,  $Q_2$  and  $Q_{hold}$  be the nominal capacity, capacity exchanged before, after and during the V-hold respectively (see Fig. 1a for a visual representation). The capacity during the V-hold can be represented as the sum of irreversible,  $Q_{irr}$  and reversible contributions,  $Q_{rev}$ :

$$Q_{hold}(t) = Q_{irr}(t) + Q_{rev}(t) = at^p + \frac{Q_{rev}^{final}(c + t_{final})t}{t_{final}(c + t)} \quad [1]$$

$$Q_{hold}^{final} = Q_{irr}^{final} + Q_{rev}^{final} \quad [2]$$

Hold current is obtained from the capacity model fit through:

$$\begin{aligned} i_{hold}(t) &= \frac{dQ_{hold}(t)}{dt} = \frac{dQ_{irr}(t)}{dt} + \frac{dQ_{rev}(t)}{dt} \\ &= pat^{p-1} + \frac{Q_{rev}^{final}(c + t_{final})c}{t_{final}(c + t)^2} \end{aligned} \quad [3]$$

While  $Q_{irr}$  shows the power law dependence on time, the form of reversible capacity,  $Q_{rev}$ , is chosen to replicate the plateauing behavior of reversible lithiation of Si as the V-hold time increases.<sup>83,84</sup> Here,  $Q_{hold}^{final}$ ,  $Q_{irr}^{final}$ ,  $Q_{rev}^{final}$  are the cumulative hold, irreversible, and reversible capacities exchanged by the end of V-hold time duration,  $t_{final}$ , respectively. For an assumed value of  $p = 0.5$  obtained from physics-based models of SEI growth, the number of unknowns decrease to 3:  $a$ ,  $Q_{rev}^{final}$  and  $c$ .

The capacities before and after the V-hold can be correlated to the reversible lithiation and irreversible parasitic capacity components during V-hold and the apparent capacity loss related to hysteresis,  $Q_{hys}$ . The anode is getting lithiated during CC as well as the CV portions. For our Si-LFP cells with an oversized cathode

(N:P  $\ll$  1) and flat cathode OCP, an excess of Li inventory is present. Any loss in lithium inventory due to the parasitic reactions will be covered by the surplus of Li present and hence the anode delithiation capacity after V-hold should not be impacted by the irreversible Li loss to the SEI:

$$Q_2 = Q_1 + Q_{rev}^{final} - Q_{hys} \quad [4]$$

If the cell showcases severe capacity losses in the formation and V-hold, even the large Li inventory can get extinguished resulting in low capacities in the cycle after the hold such that:

$$Q_2 = Q_1 + Q_{rev}^{final} - Q_{irrev}^{final} - Q_{hys}$$

Finally, the irreversible portion can be estimated for full cells by:

$$Q_{irrev}^{final} = Q_{hold}^{final} - Q_{rev}^{final} = at_{final}^p \quad [5]$$

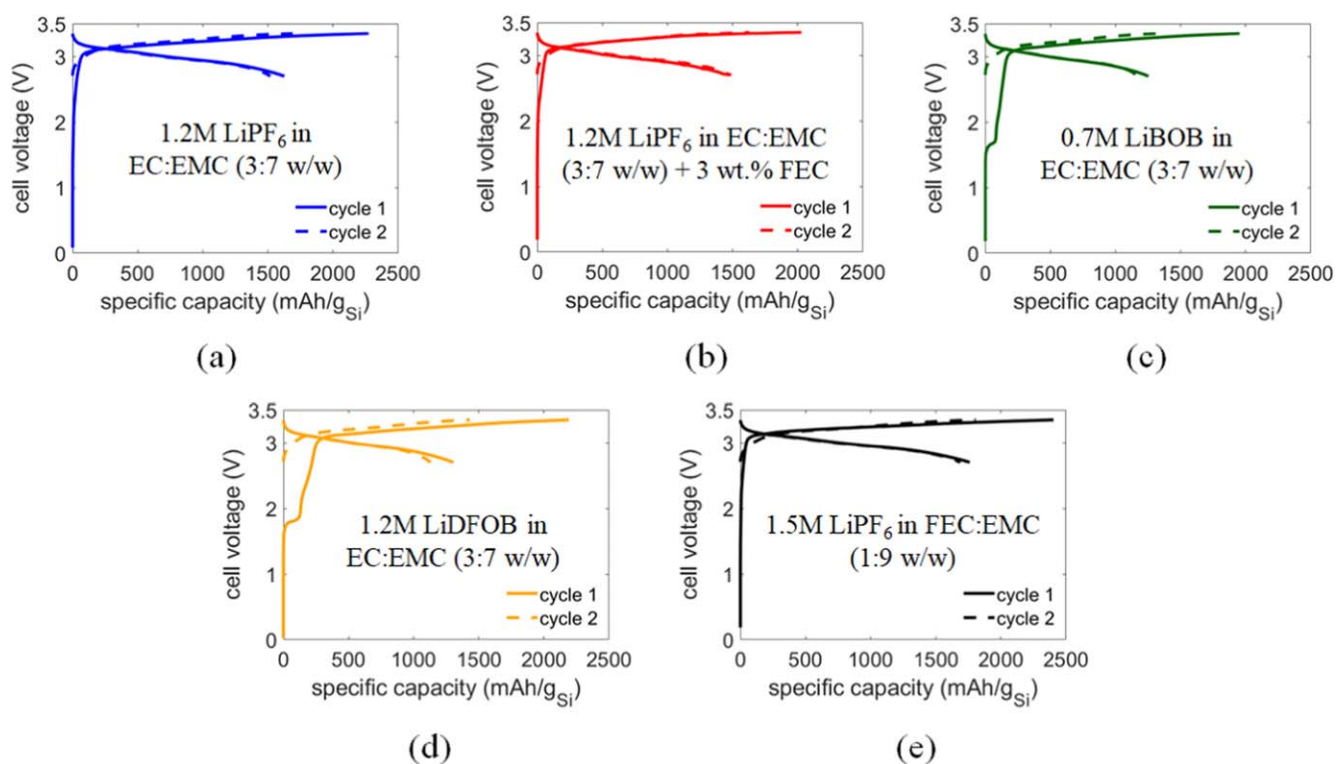
All optimization has been performed using the MATLAB curve fitting toolbox.<sup>85</sup>

## Results and Discussion

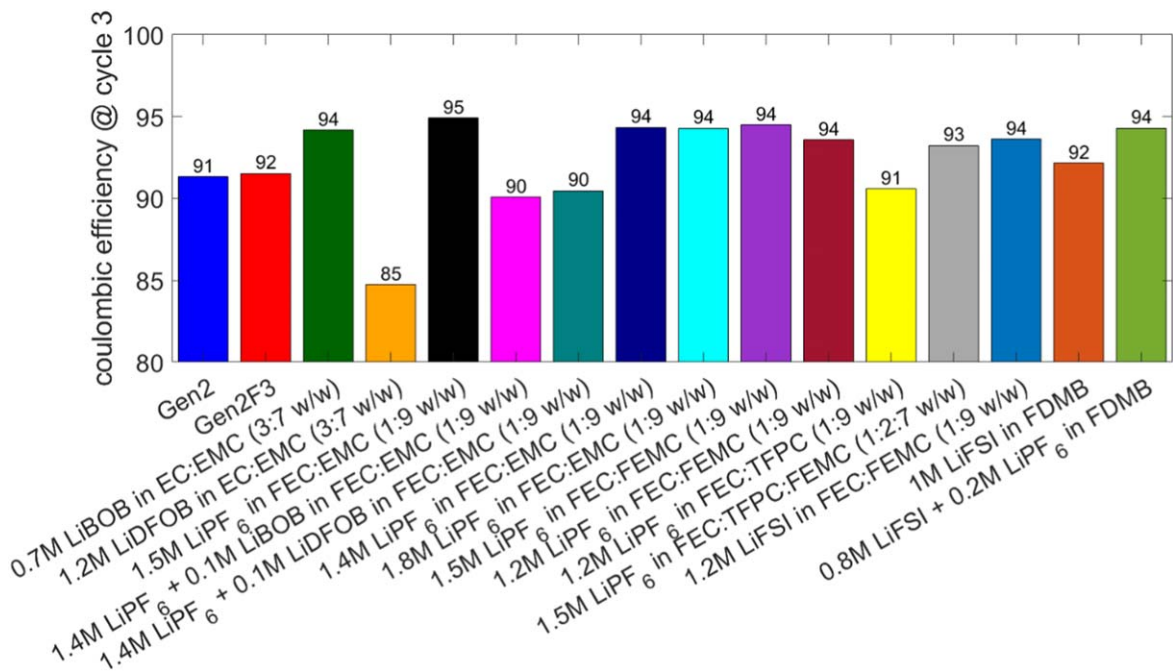
**Calendar life analysis.—Formation cycles.**—Figures 2a–2e shows the electrochemical performance, voltage vs specific capacity, during the first and second formation cycles for all the Si/LFP cells with electrolytes (1)–(5) tested using the V-hold protocol. Remaining electrolyte data is shown in Fig. S1. Upon assembly, the pristine cells have initial voltages in the 0.0 to 0.185 V range indicating completely delithiated state of silicon. During the first charge, Si lithiation is accompanied by reduction of electrolyte salt and solvents to form the SEI. 1st charge capacities above 2000 mAh/g<sub>Si</sub> are observed for all electrolytes except for 0.7 M LiBOB in EC:EMC (3:7 w/w). The presence of voltage plateaus outside the cell's normal operating window of 2.7–3.35 V gives us a clear electrochemical signature of SEI formation potentials. This is evident for the electrolytes containing LiBOB and LiDFOB salts

and can be seen in Figs. 2c & 2d. The plateaus are more prominent in Figs. 2c & 2d, where the LiBOB and LiDFOB salt are used as the primary salt as compared to when they are used as additives alongside LiPF<sub>6</sub> in Figs. S1a & S1b. LiBOB plateau occurs around a Si/LFP cell voltage of 1.63–1.67 V while the LiDFOB plateau lies in the 1.8–1.83 V full cell voltage range. Note S1, Figs. S2–S5 shows the incremental capacity analysis of all electrolytes in the 1st cycle where we can observe the dQ/dV peaks for LiBOB and LiDFOB. Given that LFP potential plateau lies around 3.40–3.46 V, this can be used to deduce a Si anode potential of 1.79–1.83 V for LiBOB salt reduction, 1.63–1.66 V for LiDFOB salt reduction vs Li.<sup>82</sup> Literature suggests that LiBOB decomposes around 1.7–1.75 V vs Li/Li<sup>+</sup> and 1.8 V for LiDFOB electrolyte.<sup>73,74,86</sup> For the remaining electrolytes, we don't see a distinct salt/solvent reduction plateau in the cell voltages during the first charge due to possible overlap of SEI reduction and Si lithiation potentials. Literature reports reduction potentials of EC, FEC around 0.6–0.8 V, 0.9–1.1 V respectively vs Li/Li<sup>+</sup>.<sup>87–89</sup> With novel solvents like FEMC, TFPC a wide range of reduction potentials are predicted. Reduction potential of FEMC is higher than that of EMC and can show multiple reduction potentials of 0.4 V, 0.78 V and 2.28 V vs Li/Li<sup>+</sup>.<sup>76,90</sup> DFT simulations show TFPC reduction in the 1.89 V–2.05 V range.<sup>78</sup> FDMB is used to increase both stability against highly reducing anode and oxidative durability against the cathode.<sup>91</sup>

Discharge capacities in the 1st cycle range from 1252–1823 mAh/g<sub>Si</sub> for the cells. Low capacities are seen for the LiBOB and LiDFOB primary salt cells: 1252 and 1303 mAh/g<sub>Si</sub>, respectively. High values are observed for the EC free 1.5 M LiPF<sub>6</sub> in FEC:EMC (1:9 w/w) and 1.5 M LiPF<sub>6</sub> in FEC:TFPC (1:9 w/w) electrolytes, 1760 and 1823 mAh/g<sub>Si</sub>, respectively. Next, we track the 1st cycle coulombic efficiencies (CEs) which is a dominant contributor to the lithium loss to the SEI as the interphase forms for the first time. The EC free FEC:EMC electrolytes consistently show CEs > 71% with 1.5 M > 1.4 M > 1.8 M. Of the EC containing formulations, LiBOB and LiDFOB electrolytes show lowest numbers ~64% and 59% respectively. There is substantial loss of 600–900 mAh/g<sub>Si</sub> capacities to the SEI in the 1st cycle. Post the 1st cycle, the losses decrease as



**Figure 2.** Cell voltage during first two formation cycles of all electrolyte systems (1)–(5) listed in Table I. Voltage plateau related to SEI formation is visible in LiBOB and LiDFOB electrolytes.



**Figure 3.** Coulombic efficiency of last formation cycle for all electrolytes.

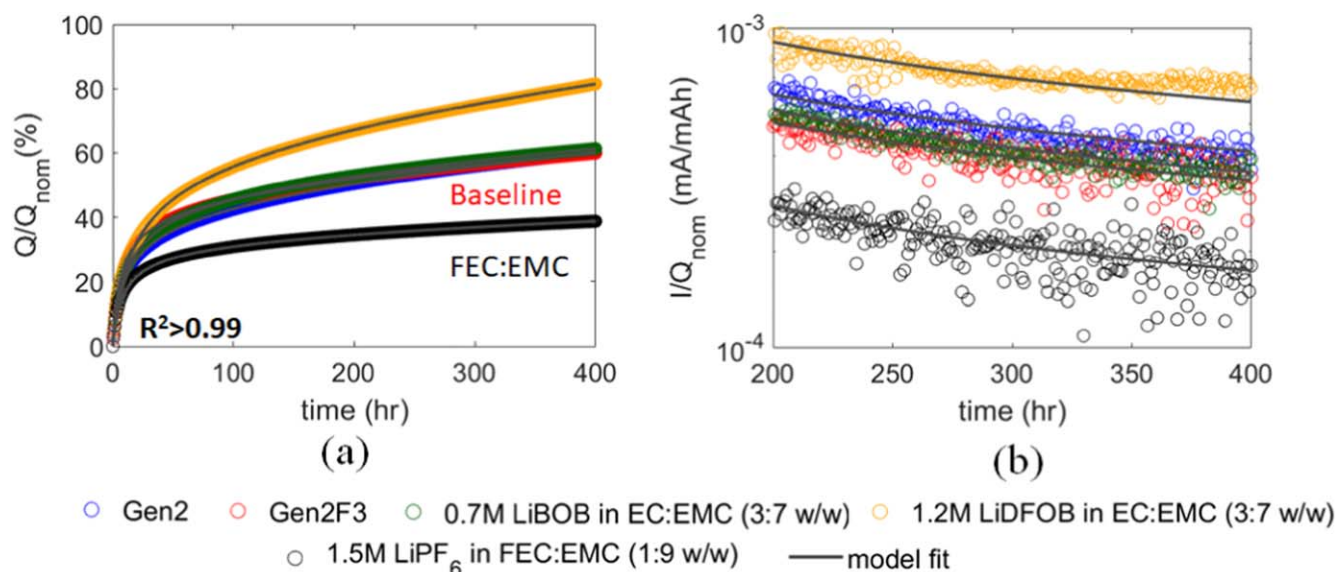
the SEI stabilizes with CEs > 90% in the final formation cycle for all electrolytes except the 1.2 M LiDFOB in EC:EMC (3:7 w/w) system (see Fig. 3).

**Voltage-hold cycle.**—We perform calendar life comparison in four sets of electrolytes and end with cycle life and oxidative stability tests on our best performing systems. The electrolyte sets are grouped according to the following themes: (1) improving over baseline electrolyte using novel EC free electrolytes, (2) variation of salt concentration and additives in the novel EC free electrolyte, (3) variation of cosolvent fluorination in the novel EC free electrolyte, and (4) moving from ester to ether solvents and LiFSI salts. The plots for each electrolyte set follow the same format, hence we keep

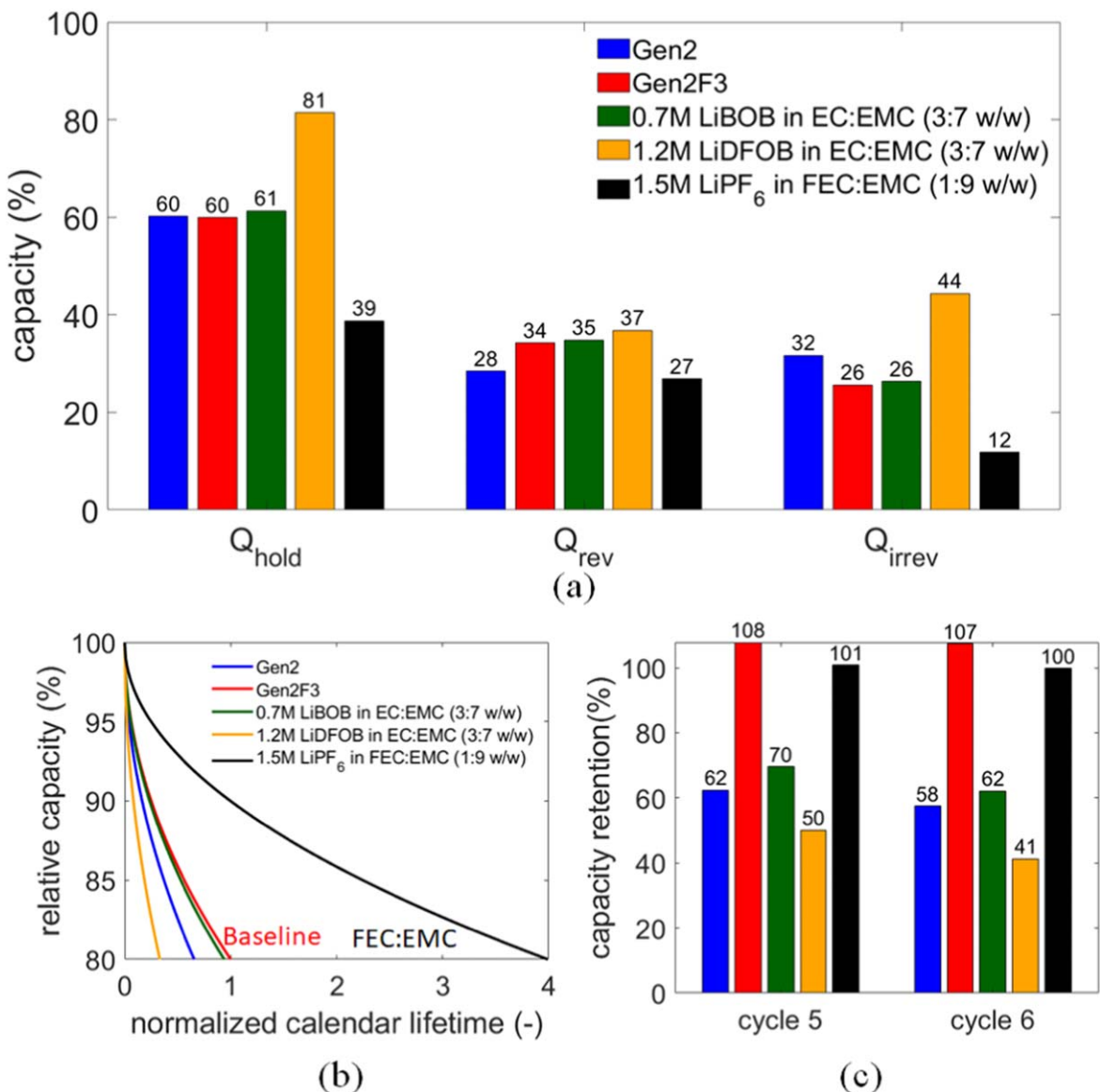
the plots for the first two electrolyte sets in the Main and keep the rest in the SI.

#### Improving over baseline electrolyte using EC free electrolytes

Figure 4a shows the temporal evolution of the experimental (symbols) capacity exchanged during the 400-hour voltage holds for electrolytes<sup>1-5</sup> in Table I. The corresponding current evolutions for latter 200 h of hold are shown in Fig. 4b. Capacity, currents are normalized with respect to the nominal discharge capacity,  $Q_{nom}$ , before the hold (in cycle 3) to enable standardized comparison across the five electrolyte systems. The model fits to the capacity and current data are shown as black lines. A good match between model and experiments is obtained with low residuals. All the fits show a good agreement with experiments for  $p = 0.5$ , indicating a diffusion



**Figure 4.** Normalized experimental electrochemical data (symbols) and deconvolution model fits (lines) during 400 hr long voltage holds on Si-LFP cells comparing baseline electrolytes with novel systems: (a) full capacity vs time, (b) zoomed current vs time for latter 200 h. The electrolytes shown are baseline electrolytes (Gen 2, Gen 2F3), LiBOB, LiDFOB in EC:EMC respectively and EC free LiPF<sub>6</sub> in FEC:EMC electrolyte. EC free FEC:EMC system shows the least capacity exchanged during the voltage hold.



**Figure 5.** (a) Comparison of hold capacity and deconvoluted reversible, irreversible capacities for baseline electrolytes, Gen 2, Gen 2F3, with LiBOB and LiDFOB in EC:EMC electrolytes and EC free LiPF<sub>6</sub> in FEC:EMC electrolyte. EC free system shows the least irreversible capacity. (b) Calendar lifetime estimates from extrapolation of irreversible capacity from model fits, (c) Discharge capacity retention of the electrolytes for cycles after voltage hold normalized to nominal discharge capacity.

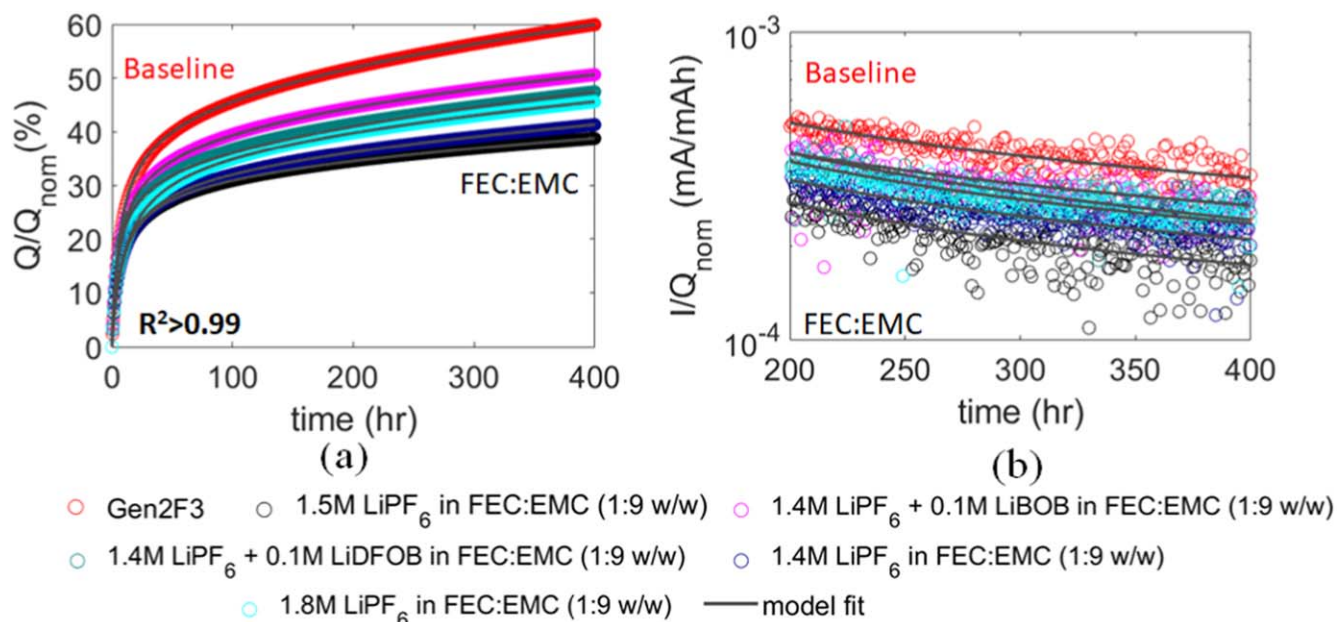
dominated growth of the SEI. Note S2, Figs. S6–S10 show the fits and residuals in more detail.

Gen2, baseline Gen2F3 and LiBOB electrolyte show similar total normalized capacity exchanged during the V-hold (~60%). LiDFOB electrolyte has the largest capacity exchanged during the V-hold (~81%), while EC free LiPF<sub>6</sub> in FEC:EMC electrolyte shows the least capacity rise (~39%). This indicates that the LiDFOB electrolyte may be a bad electrolyte choice for calendar life, while LiPF<sub>6</sub> in FEC:EMC shows promise for extension of calendar life over baseline electrolyte. The trends are mirrored in the current during V-hold plots. The lowest current during V-hold is for the EC free FEC:EMC electrolyte system. Fluorine containing salt LiDFOB has larger currents than the baseline LiPF<sub>6</sub> system, while fluorine-free LiBOB salt has similar performance to the baseline LiPF<sub>6</sub> salt.

Figure 5a shows the deconvoluted reversible and irreversible capacities for this electrolyte set. Of the 60% capacity exchanged for Gen 2 and Gen 2F3 during the hold, the split between reversible and irreversible capacities are 28%, 32% for Gen 2 and 34%, 26% for Gen2F3. Evidently, addition of FEC cosolvent to the EC:EMC

mixture lowers the parasitic losses to the SEI from 32% to 26%. F-free LiBOB salt-based electrolyte has similar performance to baseline Gen2F3 with its reversible and irreversible proportions lying at 35% and 26% respectively. LiDFOB electrolyte shows high reversible lithiation during the hold (37%), but it also has the highest irreversible capacities during the hold (44%) indicating worst SEI performance amongst this set. Irreversible capacities are at 12% for the novel EC free 1.5 M LiPF<sub>6</sub> in FEC:EMC (1:9 w/w) system, the lowest amongst these five electrolytes. Gen 2, Gen 2F3 and LiBOB electrolyte have more than double the parasitic proportion while LiDFOB electrolyte has nearly four-fold the parasitic capacity of the novel EC free electrolyte. These results indicate that replacing the primary solvent EC in the baseline electrolyte with FEC is a promising pathway to improve calendar life. The importance of accurate V-hold deconvolution is also highlighted by the fact that the seemingly equal capacities exchanged during the hold (60%) lead to different SEI performance for the Gen 2 and Gen2F3 electrolyte. Without proper deconvolution and by just looking at the V-hold capacities, we could have erroneously concluded that both





**Figure 6.** Normalized experimental electrochemical data (symbols) and deconvolution model fits (lines) during 400 hr long voltage holds on Si-LFP cells with variation of salt additives and salt concentration for the best EC free FEC:EMC system: (a) full capacity vs time, (b) zoomed current vs time for latter 200 h. The electrolytes shown are baseline Gen2F3 system, 1.5 M LiPF<sub>6</sub> in FEC:EMC, 1.4 M LiPF<sub>6</sub> with 0.1 M salt additives LiBOB, LiDFOB respectively, and 1.4 M, 1.8 M LiPF<sub>6</sub> in FEC:EMC. All variations of the FEC:EMC electrolyte show lower capacity and currents than the baseline electrolyte.

electrolytes perform the same. The model can capture the division of hold capacity into reversible and irreversible proportions allowing for correct delineation of the better Gen2F3 electrolyte.

Extrapolations of the parasitic capacity model fits to 20% capacity fade, allows us to get a semiquantitative estimate of how much better one electrolyte is as compared to the other (see Fig. 5b). V-holds are accelerated degradation tests; hence they give conservative estimates of quantitative lifetime as compared to OCV-RPT tests. So, we present the semi-quantitative version of betterment of calendar lifetime with the novel EC free FEC:EMC electrolyte. To get normalized lifetime, lifetime values of all electrolytes are divided by the calendar life of baseline Gen2F3 electrolyte. EC free FEC:EMC electrolyte outperforms the baseline Gen2F3 electrolyte in calendar life by nearly 400%. LiBOB electrolyte performs similar in calendar life to the baseline electrolyte, while LiDFOB electrolyte is worse than baseline. FEC is important and better than EC as the primary solvent for calendar life with silicon at 30 °C. Figure 5c shows the capacity retention in the reference performance test cycles 5 and 6 after the voltage hold cycle (cycle 4). Another signature of good calendar life with FEC solvent is the >100% capacity retention for the baseline Gen2F3 electrolyte and EC free 1.5 M LiPF<sub>6</sub> in FEC:EMC (1:9 w/w) system. This is possible due to the low N/P ratio of 1:3 giving excess lithium inventory. So, if there is only loss of lithium to the SEI during the V-hold protocol, the excess Li inventory makes up for good consistent capacities in cycles 5 and 6 after the hold such that the capacity retention remains close to 100%. All remaining electrolytes show <100% capacity retention indicating that poorly performing electrolytes also have other degradation modes other than LLI. A common loss mechanism with silicon is loss of active material due to fracture leading to particle isolation. We have excess electrolyte in the cells, hence other mechanisms for capacity loss like electrolyte dry out is not likely. Since the capacities in cycles 5 and 6 have dropped significantly in the 40%–70% range, we can ascribe that to loss of silicon active material with a good degree of confidence. LiDFOB electrolyte exhibits the least capacity confirming its spot as the worst electrolyte in this set. Calendar aging is typically associated with LLI, so LAM is a clear indicator of the poorest performing electrolytes.<sup>27</sup> Our Si anode material shows a mean particle size around 150 nm, which is at the critical size threshold of fracture.<sup>18</sup> While the nanosized Si

material is the same across all electrolyte sets, the variation in electrolytes can lead to diverse SEI mechanical characteristics. A mechanically robust SEI can delay silicon particle fracture while a brittle SEI can rupture and lead to subsequent Si particle cracking.<sup>13,92,93</sup> This mode of degradation can be thought of as loss of lithium inventory to the SEI inducing a loss of active material of the Si. While LAM has not been explicitly accounted for in the deconvolution, we mimic it in the model through consideration of large reduction in Li inventory such that the capacity after the hold is lower than the capacity before the hold. This leads to lower accuracy in the calendar life estimates of the worse performing electrolytes with LAM. Nevertheless, since we are concerned with finding the best performing electrolytes during the holds, the deconvolution model is accurate for these systems that predominantly showcase LLI.

For any subsequent calendar life screening with different electrolyte sets in the rest of the article, we pitch them against the Gen2F3 and EC free 1.5 M LiPF<sub>6</sub> in FEC:EMC (1:9 w/w) electrolytes to have a consistent comparison with respect to the baseline and best electrolyte respectively.

*Variation of salt concentration and additives in the novel EC free electrolyte*

Figure 6a shows the 400 h V-hold capacity exchanged evolution for the next set of EC free electrolytes (6)–(9) in Table I. The corresponding current evolutions for latter 200 h of hold are shown in Fig. 6b. Capacity, currents are normalized with the nominal discharge capacity,  $Q_{nom}$ , before the hold (in cycle 3) to enable standardized comparison across the six electrolyte systems. The model fits to the capacity and current data are shown as black lines. Again, a good match between model and experiments is obtained with low residuals. All the fits except for the electrolyte with LiBOB additive show a good agreement with experiments for  $p = 0.5$ , indicating a diffusion dominated growth of the SEI. LiBOB electrolyte shows a sub square root of time parasitic capacity growth with  $p = 0.35$ . Note S2, Figs. S11–S14 show the fits and residuals in more detail.

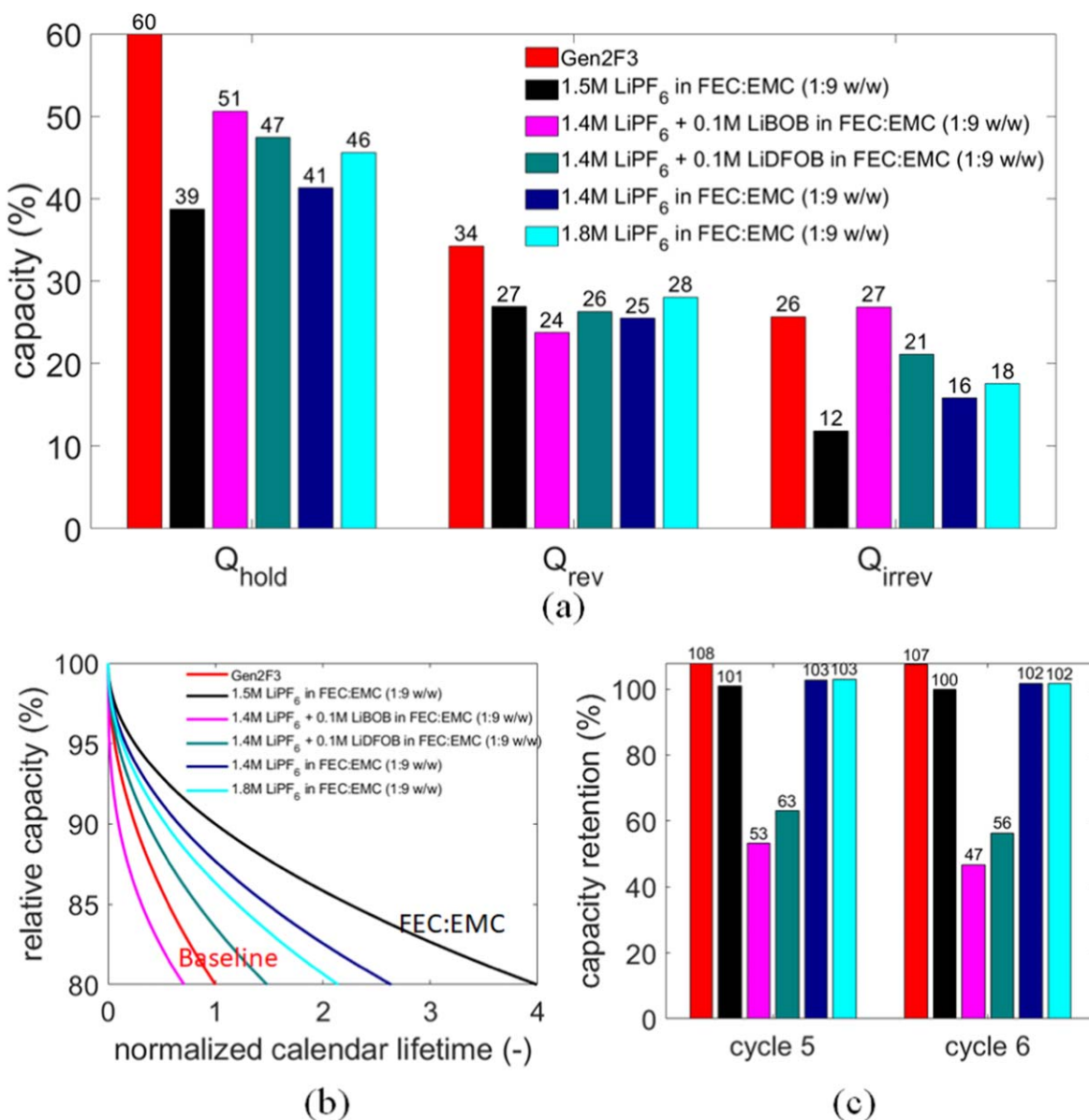
Gen 2F3 and 1.5 M LiPF<sub>6</sub> in FEC:EMC (1:9 w/w) have the highest and least capacity exchanged during the hold: 60% and 39% respectively. All other variations on the EC free system have capacities at the end of 400 h lying in between these two extremes.

Electrolytes with LiBOB and LiDFOB additives have 51% and 47% normalized capacities respectively at the end of the hold. Varying the salt concentration of pure  $\text{LiPF}_6$  in FEC:EMC to 1.4 M and 1.8 M results in final capacities at the end of the hold of 41% and 46% respectively. They show the next lowest final capacity magnitudes after the pure 1.5 M  $\text{LiPF}_6$  system. The current trends reflect the capacity profiles with least values for the pure  $\text{LiPF}_6$  in FEC:EMC system ( $1.5 \text{ M} < 1.4 \text{ M} < 1.8 \text{ M}$ ) and highest for Gen2F3. LiBOB and LiDFOB additive electrolytes have current values lying in between pure  $\text{LiPF}_6$  electrolytes and Gen2F3.

Figure 7a shows the distribution of reversible and irreversible capacities for this electrolyte set. The split of reversible and irreversible capacities is 24/27%, 26/21%, 25/16%, 28/18% for the 0.1 M LiBOB, LiDFOB additive electrolytes and pure 1.4 M  $\text{LiPF}_6$ , 1.8 M  $\text{LiPF}_6$  electrolytes respectively. LiBOB additive worsens the performance of the EC free electrolyte even below baseline Gen2F3 system. Another important result here is that while the total capacity exchanged is higher for Gen2F3 (60%) as compared to LiBOB (51%), reversible lithiation has higher proportion in the former than

the latter (34% vs 24%), resulting in higher parasitic capacity for LiBOB. Again, this highlights that we should not directly compare performance based on capacity exchanged during the hold and perform accurate deconvolution to split the irreversible part. LiDFOB additive improves the performance of EC free system over baseline but it is worse than that of pure  $\text{LiPF}_6$  in FEC:EMC system. This implies that binary salt mixtures of  $\text{LiPF}_6$  with LiBOB, LiDFOB are not particularly good for Si calendar life. In the EC free pure  $\text{LiPF}_6$  with FEC:EMC system, salt concentration has a significant impact on the SEI with the parasitic capacity trend being  $1.5 \text{ M} < 1.4 \text{ M} < 1.8 \text{ M}$ . This indicates the role of anion reduction in forming the SEI.

Figure 7b extrapolates the parasitic capacity model fits to 20% capacity fade to get a semiquantitative comparison of calendar life across this electrolyte set. Pure  $\text{LiPF}_6$  in FEC:EMC(1:9 w/w) outperforms baseline Gen2F3 electrolyte calendar life by 210/260/400% depending on salt concentrations of 1.4 M/1.8 M/1.5 M respectively. Mixing LiBOB/LiDFOB salt additives with  $\text{LiPF}_6$  worsens calendar life as compared to pure  $\text{LiPF}_6$  system. Capacity



**Figure 7.** (a) Comparison of hold capacity and deconvoluted reversible, irreversible capacities for baseline Gen 2F3 electrolyte and EC free  $\text{LiPF}_6$  in FEC:EMC electrolytes with salt additives and concentration variations. All variations of  $\text{LiPF}_6$  in EC free EMC:FEC electrolytes have lower irreversible capacities than the baseline electrolyte with the exception of LiBOB additive electrolyte. (b) Calendar lifetime estimates from extrapolation of irreversible capacity from model fits, (c) Discharge capacity retention of the electrolytes for cycles after voltage hold normalized to nominal discharge capacity.

retention in RPT cycles 5 and 6 after the V-hold cycle are shown in Fig. 7c. Baseline Gen2F3 and pure LiPF<sub>6</sub> in FEC:EMC electrolytes show >100% capacity retention indicating stable behavior of the silicon electrode itself in these electrolytes. For the electrolytes containing the LiBOB and LiDFOB additives, the reversible electrode capacity drops to 40%–60% range, indicating that some active material is being lost due to the presence of the salt additives.

#### Variation of cosolvent fluorination in the novel EC free electrolyte

Next, we screen a set of fluorinated cosolvent electrolytes with FEC as the common solvent in the EC free system. Figure S15a shows the 400 h V-hold capacity exchanged evolution for these electrolytes (10)–(13) in Table I. The corresponding current evolutions for latter 200 h of hold are shown in Fig. S15b. All the model fits (shown in black) show good agreement with experiments for  $p = 0.5$ , indicating a diffusion dominated growth of the SEI. An interesting feature of the 1.2 M LiPF<sub>6</sub> in FEC:FEMC is the flatlining in capacity and currents after ~276 h. This is indicative of channel issues, however, we are able to make a fit keeping  $t_{final}$  as 276 h, and able to get a good match between experimental data and model fit. This also revealed that we can get a good fit even after there is loss of data if there is sufficiently long V-hold capacity data to capture the reversible lithiation and irreversible parasitic current signatures. Figures S16–S19 show the fits and residuals in more detail.

FEMC is a linear molecule with 3 F atoms, while TFPC is a cyclic molecule with 3 F atoms. Binary solvent electrolytes with FEC:FEMC and 1.2 M/1.5 M LiPF<sub>6</sub> show 44%/42% total capacity exchanged during the hold. This is less than the 60% for baseline Gen2F3 but more than the 39% for 1.5 M LiPF<sub>6</sub> in FEC:EMC (1:9 w/w). Binary FEC:TFPC solvent electrolyte has the highest 72% total capacity exchanged while addition of FEMC to make it a ternary solvent mixture drops the capacity back down to 47%. Currents during the hold follow the capacity trend.

Figure S20a shows the distribution of reversible and irreversible capacities for this electrolyte set. The split of reversible and irreversible capacities is 26/18%, 24/18%, 22/49%, 27/20% for the 1.5 M, 1.2 M FEC:FEMC, FEC:TFPC and FEC:TFPC:FEMC electrolytes respectively. It is evident that not all solvent fluorination is good. Linear FEMC cosolvent with 3 F atoms paired with FEC shows the next lowest parasitic capacity (18%) after FEC:EMC (12%). Hence, it can improve calendar life over baseline Gen2F3 electrolyte but performs worse than EC free FEC:EMC electrolyte. Cyclic TFPC solvent with 3 F atoms paired with FEC shows the highest parasitic capacity (47%); it is worse than baseline Gen2F3. It is interesting that the highly fluorinated TFPC cosolvent can nullify the beneficial impact of FEC solvent and lead to a non-passivating SEI. In SEI literature, increasing electrolyte fluorination to form a LiF dominant SEI has been proposed.<sup>94</sup> LiF has poor electronic conduction which is hypothesized to increase SEI passivation. The high parasitic capacities of FEC:TFPC electrolyte indicate that not all fluorination leads to a well behaved SEI.

Figure S20b extrapolates the parasitic capacity model fits to 20% capacity fade to get a semiquantitative comparison of calendar life with cosolvent fluorination. Binary solvent FEC:FEMC electrolytes improve calendar life by 50%–70% depending on LiPF<sub>6</sub> salt concentration as compared to baseline Gen2F3 system. Highly fluorinated cyclic carbonate TFPC is a bad co-solvent and worsens calendar life severely as compared to baseline EC containing electrolyte. The addition of FEMC to make a ternary FEC:TFPC:FEMC solvent mix restores the good passivation indicating FEMC to be a good actor and TFPC to be a bad actor for Si calendar life. Capacity retention in RPT cycles 5 and 6 after the V-hold cycle are shown in Fig. S20c. All fluorinated cosolvent electrolytes show >100% capacity retention except the FEC:TFPC electrolyte, though capacity retention is still quite good at 98% indicating the parasitic capacity measured during the voltage hold is dominated by irreversible loss of lithium inventory rather than active material loss. FEMC cosolvent is a suitable candidate for good SEI

passivation on silicon after EMC. This is useful for pairing with high voltage cathodes where FEMC would have better oxidative stability as compared to EMC.<sup>76</sup>

#### Moving from ester to ether solvents and LiFSI salts

Paired with LiFSI salt, ether electrolytes showcase better reductive stability against next generation anodes.<sup>95</sup> Hence, the next electrolyte set investigates the impact of LiFSI salt and FDMB ether electrolyte on Si calendar life. Figure S21a shows the evolution of exchanged capacity during 400 h V-hold for these electrolytes (14)–(16) in Table I. The corresponding current evolutions for latter 200 h of hold are shown in Fig. S21b. All the model fits (shown in black) show good agreement with experiments for  $p = 0.5$ , indicating a diffusion dominated growth of the SEI except for LiFSI in FDMB ether solvent.  $p = 0.36$  is obtained for this electrolyte indicating a sub square root of time SEI growth. Another interesting observation here is the flatlining of capacities and currents for 1.2 M LiFSI in FEC:FEMC after ~272 h. We postulate that this is because of channel issues and can perform our model fit using a  $t_{final}$  of 272 h and obtain a good match between the data and fit. This is similar to the 1.2 M LiPF<sub>6</sub> in FEC:FEMC electrolyte which we described in the previous electrolyte set and had a flatlining around the 276 hour limit. Figures S22–S24 show the fits and residuals in more detail.

Pure LiFSI salt in FEC:FEMC and FDMB solvents exchange less capacity during the V-hold (40%, 43%) as compared to baseline Gen2F3 electrolyte (60%). Dual salt combination of 0.8 M LiFSI and 0.2 M LiPF<sub>6</sub> also shows lower capacity exchanged during the hold (47%) as compared to Gen2F3. However, the LiFSI electrolytes have higher capacity exchanged as compared to the best performing EC free LiPF<sub>6</sub> in FEC:EMC electrolyte. Of note is the comparison between LiPF<sub>6</sub> and LiFSI salts in FEC:FEMC. They show very similar capacity exchanged values of 42% and 40% respectively indicating equivalence in their electrochemical performance. Currents during the hold follow the capacity trend.

Figure S25a shows the split of reversible and irreversible capacities for this electrolyte set. The split of reversible and irreversible capacities is 25/18%, 24/16%, 28/15%, 31/16% for the LiPF<sub>6</sub> in FEC:FEMC, LiFSI in FEC:FEMC, LiFSI in FDMB and dual salt LiFSI, LiPF<sub>6</sub> in FDMB electrolytes respectively. Substituting the LiPF<sub>6</sub> salt with LiFSI in FEC:FEMC solvent shows a slight decrease in parasitic capacities. Pairing the LiFSI salt with ether FDMB solvent results in a minor lowering in irreversible capacities from the ester FEC:FEMC solvent. Dual salt combination of LiPF<sub>6</sub> and LiFSI salt in FDMB increases the parasitic capacities and does not offer any advantage over pure LiFSI in stabilizing the SEI.

Figure S25b extrapolates the parasitic capacity model fits to 20% capacity fade to get a semiquantitative comparison of calendar life with LiFSI vs LiPF<sub>6</sub> electrolytes. LiFSI in FDMB ether electrolyte improves calendar life over baseline electrolyte by nearly 3.5 times, almost as much as LiPF<sub>6</sub> in EC free FEC:EMC ester electrolyte. This is due to the slower SEI growth with  $p = 0.36$  in the ether electrolyte. This could arise from the better reductive stability at the Si anode. Mixing LiPF<sub>6</sub> and LiFSI salts in ether electrolyte or using LiFSI salt in ester carbonate electrolytes improves calendar life over baseline Gen2F3 system but does not reach the high lifetimes of the LiPF<sub>6</sub> in FEC:EMC system. Capacity retention in RPT cycles 5 and 6 after the V-hold cycle are shown in Fig. S25c. All electrolyte systems show ~100% capacity retention other than the LiFSI in FDMB. An interesting observation is that while the calendar lifetime estimates from capacity fits are good for LiFSI in FDMB, its capacity retention is the poorest amongst this set of electrolytes. It is advisable to use both metrics while downselecting the calendar life candidates.

Table III lists the fit statistics for all the electrolytes tested in this study. Good fits and low residuals are observed for all systems. Of note are the  $a$ ,  $p$  magnitudes that dictate the parasitic capacity growth. Good electrolytes with stable SEI have low  $a$  magnitudes. A

**Table III. Statistics from fits of the voltage hold data for all electrolytes.**

S. No.	Electrolyte	<i>a</i>	<i>p</i>	<i>c</i>	$Q_{rev}^{final}$ (%)	$Q_{hys}$ (%)	$R^2$ (goodness of fit)	RMSE (root mean square error)	Normalized life
1.	Gen2: 1.2 M LiPF <sub>6</sub> in EC:EMC (3:7 w/w)	1.58	0.5	9.07 (9.06, 9.08)	28.49	0.0	0.9997	0.17	0.65
2.	Gen2F3: 1.2 M LiPF <sub>6</sub> in EC:EMC (3:7 w/w) + 3 wt% FEC	1.28	0.5	6.81 (6.81, 6.82)	34.26	0.0	1	0.06	1.00
3.	0.7 M LiBOB in EC:EMC (3:7 w/w)	1.32	0.5	10.69 (10.68, 10.70)	34.79	0.0	0.9997	0.18	0.93
4.	1.2 M LiDFOB in EC:EMC (3:7 w/w)	2.23	0.5	14.02 (14.01, 14.04)	36.81	0.0	0.9996	0.28	0.33
5.	1.5 M LiPF <sub>6</sub> in FEC:EMC (1:9 w/w)	0.64	0.5	8.25 (8.25, 8.25)	25.90	1.0	0.9999	0.04	3.98
6.	1.4 M LiPF <sub>6</sub> + 0.1 M LiBOB in FEC:EMC (1:9 w/w)	3.30	0.35	5.96 (5.95, 5.97)	23.76	7.0	0.9998	0.11	0.69
7.	1.4 M LiPF <sub>6</sub> + 0.1 M LiDFOB in FEC:EMC (1:9 w/w)	1.06	0.5	4.74 (4.72, 4.76)	26.33	7.0	0.9951	0.50	1.47
8.	1.4 M LiPF <sub>6</sub> in FEC:EMC (1:9 w/w)	0.79	0.5	8.21 (8.20, 8.21)	25.49	0.0	0.9999	0.06	2.62
9.	1.8 M LiPF <sub>6</sub> in FEC:EMC (1:9 w/w)	0.88	0.5	10.34 (10.34, 10.34)	28.03	0.0	0.9999	0.07	2.13
10.	1.5 M LiPF <sub>6</sub> in FEC:FEMC (1:9 w/w)	0.96	0.5	6.23(6.21, 6.24)	25.26	0.0	0.9982	0.29	1.79
11.	1.2 M LiPF <sub>6</sub> in FEC:FEMC (1:9 w/w)	1.06	0.5	7.91 (7.90, 7.92)	24.75	1.0	0.9996	0.14	1.61
12.	1.5 M LiPF <sub>6</sub> in FEC:TFPC (1:9 w/w)	2.46	0.5	8.14 (8.09, 8.17)	22.40	2.0	0.998	0.63	0.27
13.	1.5 M LiPF <sub>6</sub> in FEC:TFPC:FEMC (1:2:7 w/w)	1.01	0.5	6.84 (6.82, 6.86)	27.29	1.0	0.9968	0.42	1.45
14.	1.2 M LiFSI in FEC:FEMC (1:9 w/w)	0.97	0.5	7.92 (7.92, 7.93)	24.26	1.0	0.9997	0.11	1.73
15.	1 M LiFSI in FDMB	1.75	0.36	8.25 (8.24, 8.26)	28.11	3.0	0.9993	0.16	3.58
16.	0.8 M LiFSI + 0.2 M LiPF <sub>6</sub> in FDMB	0.81	0.5	7.47 (7.46, 7.48)	31.04	1.0	0.9993	0.18	2.49



$p = 0.5$  indicates diffusion dominated growth of the SEI which is observed for most systems here. Electrochemical reaction limited SEI growth generally shows linear time dependence  $p = 1$ . If there is cracking and fresh SEI surfaces are exposed, a value of  $p > 0.5$  is to be expected. If the SEI is highly passivating, a value of  $p < 0.5$  can be expected.<sup>83</sup> Few electrolytes show good fits only with a non-zero hysteresis capacity which can be attributed to higher impedance in these systems.

Note S3, Figs. S26–S29 shows the incremental capacity  $dQ/dV$  profiles during the constant current portion of the V-hold cycle for all electrolytes. All electrolytes generally show one predominant peak around 3.2 V during the constant current charge. With additional reversible Si lithiation during the constant voltage hold, the better performing electrolytes show two predominant peaks related to Si delithiation during the constant current discharge (see Figs. S26b, S27a etc.). The worse performing electrolytes generally have more irreversible SEI growth than reversible lithiation during the constant voltage hold, and hence show only one peak in the constant current discharge after the hold due to less lithium inventory (see Figs. S26a, S26d etc.).

**Reference performance test cycles.**—Figures 8a–8e shows the voltage vs specific capacity during the charge and discharge for cycles before (cycle 3) and after (cycle 5) the hold for electrolytes (1)–(5). Remaining electrolyte data is shown in Fig. S30. A good electrolyte formulation results in high discharge capacity retention from cycle 3 to cycle 5. Baseline Gen2F3, EC free  $\text{LiPF}_6$  in FEC:EMC,  $\text{LiPF}_6$  in FEC:FEMC, LiFSI in FEC:FEMC and dual salt LiFSI,  $\text{LiPF}_6$  in FDMB exhibits this feature of  $>100\%$  capacity retention in cycle 5. All other electrolytes show a drop in discharge capacities in cycle 5 from cycle 3 which is an indication of loss of active material in the system. Interestingly, LAM correlates with the worst performing electrolytes for calendar life.

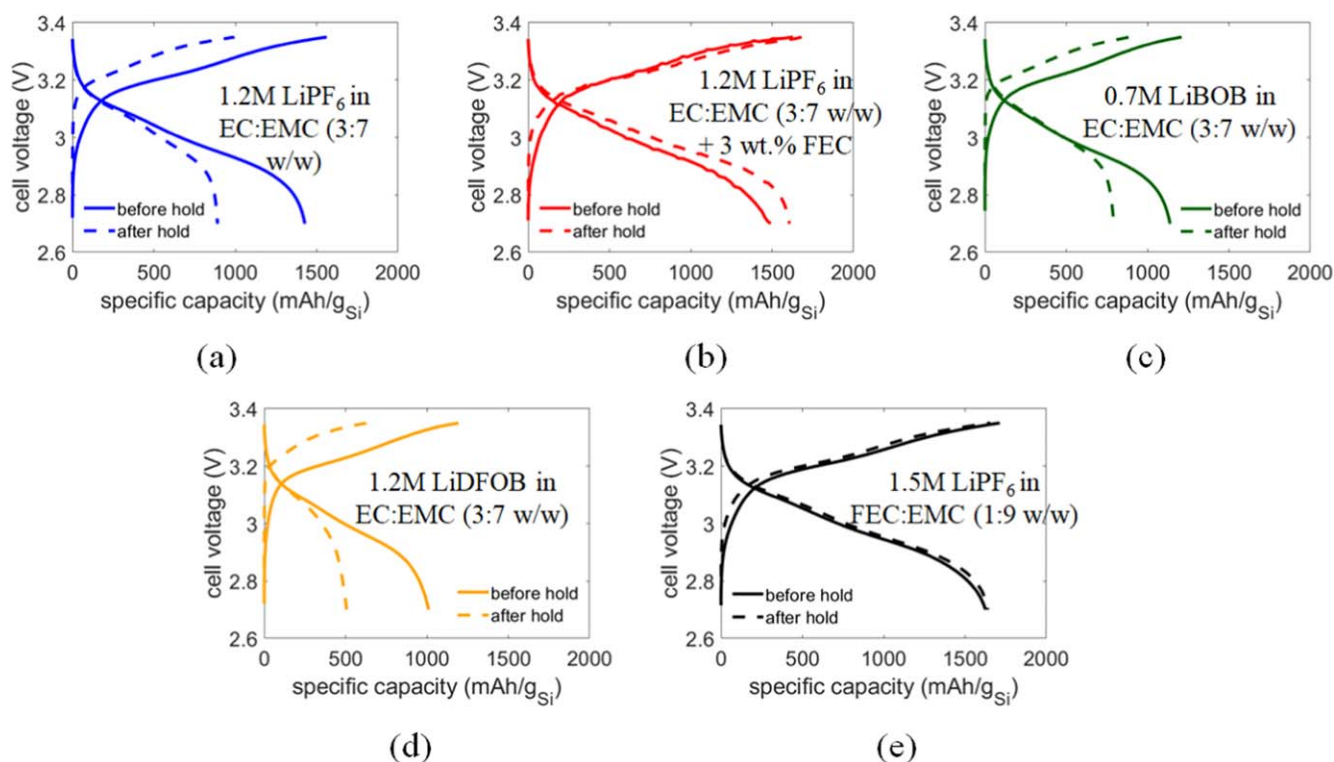
From the calendar life testing using V-hold, we can identify three potential electrolyte candidates to improve calendar lifetime of silicon:

- (1) Partially fluorinated EC free electrolyte 1.4 M/1.5 M/1.8 M  $\text{LiPF}_6$  in FEC:EMC (1:9 w/w): improves calendar life over baseline Gen2F3 by 100 to 300%.
- (2) Highly fluorinated EC free electrolyte 1.2 M/1.5 M  $\text{LiPF}_6$  in FEC:FEMC (1:9 w/w): improves calendar life over baseline Gen2F3 by 50 to 80%.
- (3)  $\text{LiPF}_6$ /EC free ether electrolyte 1 M LiFSI in FDMB: improves calendar life over baseline Gen2F3 by 250%.

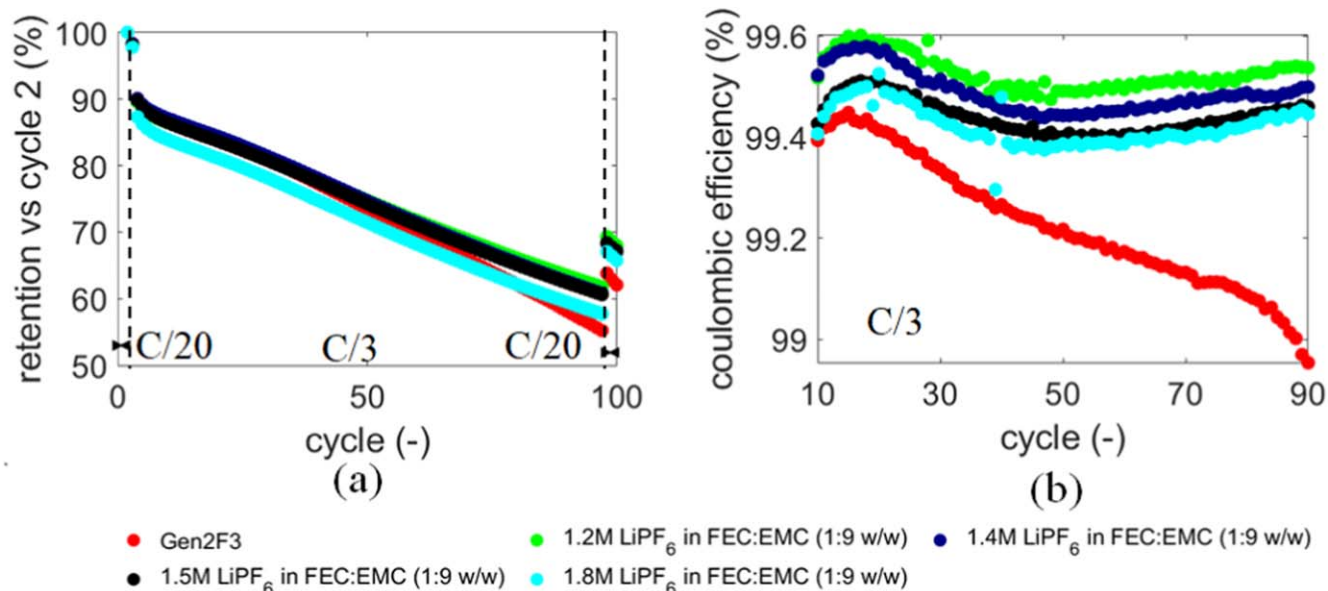
The first electrolyte eliminates EC to improve Si calendar life. The second electrolyte includes FEMC to improve reductive stability at the Si anode with respect to baseline Gen2F3 and promises better oxidative stability with high voltage NMC cathode.<sup>76</sup> The third electrolyte also shows better reduction characteristics at the Si anode while its good oxidative stability is a highlight in literature.<sup>95</sup> It is noted that the electrolyte costs are expected to increase with these novel formulations. Electrolyte cost is  $\sim 4.5\%$  of the total battery material cost with salt being the dominant contributor as compared to solvents.<sup>96</sup> Hence, we expect the cost increase to not be limiting, especially with  $\text{LiPF}_6$  based formulations where we are only swapping out the solvents.

**Cycle life analysis.**—To assess the efficacy of a new electrolyte for silicon, it should improve calendar life while not diminishing cycle life. We downselect the  $\text{LiPF}_6$  in FEC:EMC (1:9 w/w) electrolyte system to test for cycle life in the Si|NMC811 cell configuration as it showed the best promise for calendar life. Figure 9a shows the capacity retention for  $3 \times C/20$ ,  $94 \times C/3$ ,  $3 \times C/20$  cycles of Si-NMC cell with 1.2 M, 1.4 M, 1.5 M, 1.8 M  $\text{LiPF}_6$  in FEC:EMC electrolyte in comparison to baseline Gen2F3 electrolyte. Here, the retention is with respect to capacity in cycle 2. Zoomed coulombic efficiency for the cycles 10–90 with same electrolyte set are show in Fig. 9b.

Capacity retention for the EC free FEC:EMC electrolyte systems consistently lie above the baseline Gen2F3 electrolyte at the end of the 100 cycles. The final capacity retention values at the end of the



**Figure 8.** Performance curves (voltage vs specific capacity) during charge and discharge for cycles before and after voltage hold for electrolytes (1)–(5) listed in Table I. Better electrolytes show increased capacity after hold.



**Figure 9.** (a) Capacity retention for  $3 \times C/20$ ,  $94 \times C/3$ ,  $3 \times C/20$  cycles of Si-NMC cell with 1.2 M, 1.4 M, 1.5 M, 1.8 M LiPF<sub>6</sub> in FEC:EMC electrolyte and compared with baseline Gen2F3 electrolyte. (b) Zoomed capacity retention during the 1 C cycles from cycle number 10–90.

last C/20 cycle are 62%, 68%, 67%, 67% and 66% for Gen 2F3, 1.2 M, 1.4 M, 1.5 M, 1.8 M LiPF<sub>6</sub> in FEC:EMC respectively. A 4%–6% increase in capacity retention is observed for the EC free FEC:EMC system depending on the salt concentration. To understand the cause for this higher capacity retention, we investigate the coulombic efficiencies (CE) which are a signature of capacity lost to SEI in each cycle. The final CE's are 97.58%, 99.13%, 99.18%, 98.90% and 98.77% for Gen 2F3, 1.2 M, 1.4 M, 1.5 M, 1.8 M LiPF<sub>6</sub> in FEC:EMC respectively. A  $\sim 1.5\%$  higher CE is observed with the EC free FEC:EMC system depending on the salt concentration as compared to Gen2F3 at the end of 100 cycles. Another interesting observation is the CE trend with respect to cycles which is shown in Fig. 9b. Baseline Gen2F3 electrolyte shows an approximate monotonically decreasing coulombic efficiency from cycle 20 onwards. This is an indicator of non-passivating SEI where the Li inventory loss to the SEI keeps increasing as a function of cycles. A well-passivated SEI would result in stabilized numbers of CE as the SEI thickens such that there is less loss of Li to the SEI with each cycle due to longer transport distances required for the electron and Li<sup>+</sup> ions to attack the solvent. This is observed for all the FEC:EMC electrolytes. The CE profiles for all FEC:EMC electrolytes show non-monotonicity: increase in earlier cycles up to cycle 20, reduction in cycles 20–50 with subsequent increases from cycle 50 onwards indicating a good degree of passivation. The CE in cycles 10–50 also lie consistently above 99.4% for FEC:EMC electrolytes while the Gen2F3 electrolyte CE drops below 99.2% after cycle 50.

Note S4, Figs. S31–S33 show the areal capacity, specific capacity trends for cycles 1–100 and coulombic efficiency trends during cycle 1–10, 90–100. We observe higher capacities, CEs for the FEC:EMC electrolyte. To compare oxidative stability tests of this new electrolyte, we perform cyclic voltammetry on Li|Al cells between 3–5 V. As shown in Note S5, Fig. S34, EC containing baseline Gen2F3 electrolyte shows an order of magnitude higher oxidative currents as compared to novel EC free 1.2 M LiPF<sub>6</sub> in FEC:EMC (1:9 w/w) electrolyte for the entire voltage range. This suggests that the new electrolyte reacts less at the cathode surface and/or would provide better passivation at the Al current collector.

**Limitations.**—This work utilizes early life testing using V-hold protocol to estimate semiquantitative calendar lifetime of the electrolytes in the coin cell configuration with  $\sim 2$  mAh nominal capacities. Calendar and cycle life testing always give better

quantitative estimates in larger Ah cell configurations like cylindrical/pouch/prismatic cells manufactured using semiautomated assembly lines as compared to handmade coin cells.<sup>97</sup> Furthermore, the extrapolation of calendar lifetime does not account for capacity knees with long duration testing that can occur from electrolyte dryout, gas generation leading to inaccessible electrode active material etc.<sup>98</sup> Our analysis did not include LAM explicitly, which is a relevant aging mechanism for silicon, especially when the cell is cycled which happens during the reference performance tests. V-hold is fundamentally focused on getting a description of LLI but LAM for good Si samples may only kick in later in life, which would be completely missed by V-holds.

Calendar life results from V-hold tests may vary depending on the silicon anode based on surface termination or doping. If a larger sized silicon is used, the results could be dominated by fracture and loss of active material. Depending on silicon identity like Si-pitch,<sup>21</sup> Si-PEO<sup>19</sup> or B doped Si,<sup>99</sup> some differences in the result can be expected. But we expect some consistency in results across silicon and will explore it in future work. This work was focused on screening electrolytes for calendar life and rate effects were not investigated. In literature, Landesfeind and Gasteiger<sup>100</sup> have measured the transport properties (conductivity, diffusivity, transference number) of the FEC:EMC (1:19 w/w) system. At 30 °C, the EC:EMC electrolyte has a maximum conductivity  $\sim 10$  mS cm<sup>-1</sup> at 1 M salt concentration. In comparison, the FEC:EMC electrolyte has a maximum conductivity  $\sim 7.5$  mS cm<sup>-1</sup> at 1.5 M salt concentration, so it's 25% lower as compared to the baseline electrolyte. We expect more severe rate limitations with FEC:EMC as we cycle the Si cells at higher rates above 1 C.

## Conclusions and Outlook


This study utilized voltage-hold protocols on Si|LFP cells to rapidly screen sixteen electrolyte formulations for calendar life within 2 months. The EC free LiPF<sub>6</sub> in FEC:EMC (1:9 w/w) electrolyte shows consistently low parasitic SEI currents and capacities as compared to the baseline Gen2F3 LiPF<sub>6</sub> in EC:EMC: FEC electrolyte. Subsequently, model fits are used to extrapolate the lithium loss to 20% capacity fade to estimate a substantial  $>100\%$  increase in calendar life with the new electrolyte. The new electrolyte is then subjected to cycling and cyclic voltammetry tests to assess its effectiveness in improving cycle life and oxidative stability. In both these tests, the EC free system outperforms the

Gen2F3 baseline. Our approach can be utilized towards finding new electrolytes with enhanced calendar life for Si dominant anodes. This approach is extensible to next generation systems like Si with solid electrolytes. Detailed characterization using imaging and spectroscopy techniques can help answer the question as to why one electrolyte is better than the other.<sup>101</sup> Furthermore, we plan to investigate the benefits of novel EC free electrolyte in larger format cells and in traditional OCV-RPT calendar lifetime tests.

### Acknowledgments

This research was supported by the U.S. Department of Energy's Vehicle Technologies Office under the Silicon Consortium Project, directed by Brian Cunningham, Nicolas Eidson and Thomas Do, and managed by Anthony Burrell. This manuscript was created by the Alliance for Sustainable Energy, LLC, the manager, and operator of the National Renewable Energy Laboratory for the U.S. Department of Energy (DOE) under Contract No. DE-AC36-08GO28308. This work was authored in part by UChicago Argonne, LLC, Operator of Argonne National Laboratory ("Argonne"). Argonne, a U.S. Department of Energy Office of Science laboratory, is operated under Contract No. DE-AC02-06CH11357. The views expressed in the article do not necessarily represent the views of the DOE or the U.S. Government. The U.S. Government retains and the publisher, by accepting the article for publication, acknowledges that the U.S. Government retains a nonexclusive, paid-up, irrevocable, worldwide license to publish or reproduce the published form of this work, or allow others to do so, for U.S. Government purposes. The authors declare that they have no known competing financial interests or personal relationships that could have appeared to influence the work reported in this paper.

### ORCID

Ankit Verma  <https://orcid.org/0000-0002-7610-8574>  
 Maxwell C. Schulze  <https://orcid.org/0000-0001-8368-4054>  
 Andrew Colclasure  <https://orcid.org/0000-0002-9574-5106>  
 Marco-Tulio Fonseca Rodrigues  <https://orcid.org/0000-0003-0833-6556>  
 Stephen E. Trask  <https://orcid.org/0000-0002-0879-4779>  
 Krzysztof Papek  <https://orcid.org/0009-0006-9094-5340>  
 Daniel P. Abraham  <https://orcid.org/0000-0003-0402-9620>

### References

- J. T. Frith, M. J. Lacey, and U. Ulissi, *Nat. Commun.*, **14**, 420 (2023).
- J. Sturm, A. Rheinfeld, I. Zilberman, F. B. Spingler, S. Kosch, F. Frie, and A. Jossen, *J. Power Sources*, **412**, 204 (2019).
- C.-H. Chen, F. B. Planella, K. O'regan, D. Gastol, W. D. Widanage, and E. Kendrick, *J. Electrochem. Soc.*, **167**, 080534 (2020).
- A. Zülke, I. Korotkin, J. M. Foster, M. Nagarathinam, H. Hoster, and G. Richardson, *J. Electrochem. Soc.*, **168**, 120522 (2021).
- G. G. Eshetu, H. Zhang, X. Judez, H. Adenusi, M. Armand, S. Passerini, and E. Figgemeier, *Nat. Commun.*, **12**, 5459 (2021).
- A. Lahiri, N. Shah, and C. Dales, *IEEE Spectr.*, **55**, 34 (2018).
- D. Schneider, *IEEE Spectr.*, **56**, 48 (2018).
- Y. Cui, *Nat. Energy*, **6**, 995 (2021).
- M. T. McDowell, S. W. Lee, W. D. Nix, and Y. Cui, *Adv. Mater.*, **25**, 4966 (2013).
- M. Obrovac, L. Christensen, D. B. Le, and J. R. Dahn, *J. Electrochem. Soc.*, **154**, A849 (2007).
- R. Chandrasekaran, A. Magasinski, G. Yushin, and T. F. Fuller, *J. Electrochem. Soc.*, **157**, A1139 (2010).
- A. Verma, A. A. Franco, and P. P. Mukherjee, *J. Electrochem. Soc.*, **166**, A3852 (2019).
- A. Verma and P. P. Mukherjee, *J. Electrochem. Soc.*, **164**, A3570 (2017).
- D. E. Galvez-Aranda, A. Verma, K. Hankins, J. M. Seminario, P. P. Mukherjee, and P. B. Balbuena, *J. Power Sources*, **419**, 208 (2019).
- D. Anseán, G. Baure, M. González, I. Cameán, A. García, and M. Dubarry, *J. Power Sources*, **459**, 227882 (2020).
- M. P. Bonkile, Y. Jiang, N. Kirkaldy, V. Sulzer, R. Timms, H. Wang, G. Offer, and B. Wu, *J. Power Sources*, **606**, 234256 (2024).
- J. W. Choi, Y. Cui, and W. D. Nix, *Journal of the Mechanics & Physics of Solids*, **59**, 1717 (2011).
- X. H. Liu, L. Zhong, S. Huang, S. X. Mao, T. Zhu, and J. Y. Huang, *ACS Nano*, **6**, 1522 (2012).
- M. C. Schulze, F. Urias, N. S. Dutta, Z. Huey, J. Coyle, G. Teeter, R. Doeren, B. J.-T. de Villers, S.-D. Han, and N. R. Neale, *J. Mater. Chem. A*, **11**, 5257 (2023).
- M. T. McDowell, S. W. Lee, C. Wang, and Y. Cui, *Nano Energy*, **1**, 401 (2012).
- M. C. Schulze, K. Fink, J. Palmer, G. M. Carroll, N. S. Dutta, C. Zwielfel, C. Engrakul, S. D. Han, N. R. Neale, and B. J. Tremolet de Villers, *Batteries & Supercaps*, **6**, e202300186 (2023).
- S. Dalavi, P. Guduru, and B. L. Lucht, *J. Electrochem. Soc.*, **159**, A642 (2012).
- G. G. Eshetu and E. Figgemeier, *ChemSusChem*, **12**, 2515 (2019).
- S. Zhang, M. He, C.-C. Su, and Z. Zhang, *Current Opinion in Chemical Engineering*, **13**, 24 (2016).
- J. D. McBrayer, M.-T. F. Rodrigues, M. C. Schulze, D. P. Abraham, C. A. Applett, I. Bloom, G. M. Carroll, A. M. Colclasure, C. Fang, and K. L. Harrison, *Nat. Energy*, **6**, 866 (2021).
- K. Kalaga, M.-T. F. Rodrigues, S. E. Trask, I. A. Shkrob, and D. P. Abraham, *J. Electrochimica Acta*, **280**, 221 (2018).
- I. Zilberman, J. Sturm, and A. Jossen, *J. Power Sources*, **425**, 217 (2019).
- I. Zilberman, S. Ludwig, and A. Jossen, *Journal of Energy Storage*, **26**, 100900 (2019).
- E. Peled and S. Menkin, *J. Electrochem. Soc.*, **164**, A1703 (2017).
- J. D. McBrayer, K. L. Harrison, E. Allcorn, and S. D. Minter, *Frontiers in Batteries & Electrochemistry*, **2**, 9 (2023).
- G. M. Veith, M. Doucet, J. K. Baldwin, R. L. Sacci, T. M. Fears, Y. Wang, and J. F. Browning, *The Journal of Physical Chemistry C*, **119**, 20339 (2015).
- J. P. Christophersen, (2015), <https://www.osti.gov/biblio/1186745>.
- E. J. Dufek, T. R. Tanim, B.-R. Chen, and S. Kim, *Joule*, **6**, 1363 (2022).
- S. Grolleau, A. Delaille, H. Gualous, P. Gyan, R. Revel, J. Bernard, E. Redondo-Iglesias, J. Peter, and S. Network, *J. Power Sources*, **255**, 450 (2014).
- A. Zülke, Y. Li, P. Keil, R. Burrell, S. Belaisch, M. Nagarathinam, M. P. Mercer, and H. E. Hoster, *Batteries & Supercaps*, **4**, 934 (2021).
- M.-T. F. Rodrigues, Z. Yang, S. E. Trask, A. R. Dunlop, M. Kim, F. Dogan, B. Key, I. Bloom, D. P. Abraham, and A. N. Jansen, *J. Power Sources*, **565**, 232894 (2023).
- P. Gasper, N. Collath, H. C. Hesse, A. Jossen, and K. Smith, *J. Electrochem. Soc.*, **169**, 080518 (2022).
- P. Gasper, A. Saxon, Y. Shi, E. Endler, K. Smith, and F. M. Thakkar, *Journal of Energy Storage*, **73**, 109042 (2023).
- A. Tornheim, S. Sharifi-Asl, J. C. Garcia, J. Bareño, H. Iddir, R. Shahbazian-Yassar, and Z. Zhang, *Nano Energy*, **55**, 216 (2019).
- M. C. Schulze, M.-T. F. Rodrigues, J. D. McBrayer, D. P. Abraham, C. A. Applett, I. Bloom, Z. Chen, A. M. Colclasure, A. R. Dunlop, and C. Fang, *J. Electrochem. Soc.*, **169**, 050531 (2022).
- A. Verma, M. C. Schulze, A. Colclasure, M.-T. F. Rodrigues, S. E. Trask, K. Papek, C. S. Johnson, and D. P. Abraham, *J. Electrochem. Soc.*, **170**, 070516 (2023).
- S. Buechele, A. Adamson, A. Eldesoky, T. Boettcher, L. Hartmann, T. Boulanger, S. Azam, M. B. Johnson, T. Taskovic, and E. Logan, *J. Electrochem. Soc.*, **170**, 010511 (2023).
- S. Buechele, E. Logan, T. Boulanger, S. Azam, A. Eldesoky, W. Song, M. B. Johnson, and M. Metzger, *J. Electrochem. Soc.*, **170**, 010518 (2023).
- K. Xu, *Chem. Rev.*, **104**, 4303 (2004).
- K. Xu, *Chem. Rev.*, **114**, 11503 (2014).
- T. F. Malkowski, Z. Yang, R. L. Sacci, S. E. Trask, M.-T. F. Rodrigues, I. D. Bloom, and G. M. Veith, *J. Power Sources*, **523**, 231021 (2022).
- L. Lv, Y. Wang, W. Huang, Y. Wang, G. Zhu, and H. Zheng, *Electrochim. Acta*, **413**, 140159 (2022).
- G. Hernández, A. J. Naylor, Y.-C. Chien, D. Brandell, J. Mindemark, and K. Edström, *ACS Sustainable Chemistry & Engineering*, **8**, 10041 (2020).
- B. S. Parimalam and B. L. Lucht, *J. Electrochem. Soc.*, **165**, A251 (2018).
- C. C. Nguyen and B. L. Lucht, *J. Electrochem. Soc.*, **161**, A1933 (2014).
- H. Nakai, T. Kubota, A. Kita, and A. Kawashima, *J. Electrochem. Soc.*, **158**, A798 (2011).
- V. Etacheri, O. Haik, Y. Goffer, G. A. Roberts, I. C. Stefan, R. Fasching, and D. Aurbach, *Langmuir*, **28**, 965 (2012).
- A. Bordes, K. Eom, and T. F. Fuller, *J. Power Sources*, **257**, 163 (2014).
- T. Jaumann, J. Balach, M. Klose, S. Oswald, U. Langklotz, A. Michaelis, J. Eckert, and L. Giebeler, *Phys. Chem. Chem. Phys.*, **17**, 24956 (2015).
- T. Jaumann, J. Balach, U. Langklotz, V. Sauchuk, M. Fritsch, A. Michaelis, V. Teltevsikij, D. Mikhailova, S. Oswald, and M. Klose, *Energy Storage Mater.*, **6**, 26 (2017).
- H. Shobukawa, J. Alvarado, Y. Yang, and Y. S. Meng, *J. Power Sources*, **359**, 173 (2017).
- M. J. Piernas-Muñoz, Z. Yang, M. Kim, S. E. Trask, A. R. Dunlop, and I. Bloom, *J. Power Sources*, **487**, 229322 (2021).
- X. Chen, X. Li, D. Mei, J. Feng, M. Y. Hu, J. Hu, M. Engelhard, J. Zheng, W. Xu, and J. Xiao, *ChemSusChem*, **7**, 549 (2014).
- G. M. Veith, M. Doucet, R. L. Sacci, B. Vacaliuc, J. K. Baldwin, and J. F. Browning, *Sci. Rep.*, **7**, 6326 (2017).
- E. J. Hopkins, S. Frisco, R. T. Pekarek, C. Stetson, Z. Huey, S. Harvey, X. Li, B. Key, C. Fang, and G. Liu, *J. Electrochem. Soc.*, **168**, 030534 (2021).
- G. M. Veith, K. L. Browning, M. Doucet, and J. F. Browning, *J. Electrochem. Soc.*, **168**, 060523 (2021).
- R. J. Mou, S. Barua, D. P. Abraham, and K. P. Yao, *J. Electrochem. Soc.*, **171**, 040546 (2024).
- B. T. Young, D. R. Heskett, C. C. Nguyen, M. Nie, J. C. Woicik, and B. L. Lucht, *ACS Appl. Mater. Interfaces*, **7**, 20004 (2015).
- J. Kim, O. B. Chae, and B. L. Lucht, *J. Electrochem. Soc.*, **168**, 030521 (2021).
- Y. Li, Z. Cao, Y. Wang, L. Lv, J. Sun, W. Xiong, Q. Qu, and H. Zheng, *ACS Energy Lett.*, **8**, 4193 (2023).



66. Y. S. Meng, V. Srinivasan, and K. Xu, *Science*, **378**, eabq3750 (2022).
67. K. Xu, *J. Power Sources*, **559**, 232652 (2023).
68. T. Zhang and E. Paillard, *Frontiers of Chemical Science & Engineering*, **12**, 577 (2018).
69. S. Zhang, T. Jow, K. Amine, and G. Henriksen, *J. Power Sources*, **107**, 18 (2002).
70. E. W.-C. Spotte-Smith, T. B. Petrocelli, H. D. Patel, S. M. Blau, and K. A. Persson, *ACS Energy Lett.*, **8**, 347 (2022).
71. H.-B. Han, S.-S. Zhou, D.-J. Zhang, S.-W. Feng, L.-F. Li, K. Liu, W.-F. Feng, J. Nie, H. Li, and X.-J. Huang, *J. Power Sources*, **196**, 3623 (2011).
72. C. L. Berhaut, D. Lemordant, P. Porion, L. Timperman, G. Schmidt, and M. Anouti, *RSC Adv.*, **9**, 4599 (2019).
73. Y. Zhu, Y. Li, M. Bettge, and D. P. Abraham, *J. Electrochem. Soc.*, **159**, A2109 (2012).
74. K. Xu, S. Zhang, and T. R. Jow, *Electrochemical Solid-State Letters*, **8**, A365 (2005).
75. Y. Ha, D. P. Finegan, A. M. Colclasure, S. E. Trask, and M. Keyser, *Electrochim. Acta*, **394**, 139097 (2021).
76. Y.-M. Lee, K.-M. Nam, E.-H. Hwang, Y.-G. Kwon, D.-H. Kang, S.-S. Kim, and S.-W. Song, *The Journal of Physical Chemistry C*, **118**, 10631 (2014).
77. S. Yang, Y. Zhang, Z. Li, N. Takenaka, Y. Liu, H. Zou, W. Chen, M. Du, X.-J. Hong, and R. Shang, *ACS Energy Lett.*, **6**, 1811 (2021).
78. Z. Hu, L. Zhao, T. Jiang, J. Liu, A. Rashid, P. Sun, G. Wang, C. Yan, and L. Zhang, *Adv. Funct. Mater.*, **29**, 1906548 (2019).
79. Z. Yu, H. Wang, X. Kong, W. Huang, Y. Tsao, D. G. Mackanic, K. Wang, X. Wang, W. Huang, and S. Choudhury, *Nat. Energy*, **5**, 526 (2020).
80. H. S. Dhattarwal, J.-L. Kuo, and H. K. Kashyap, *The Journal of Physical Chemistry C*, **126**, 8953 (2022).
81. G. V. Zhuang, K. Xu, H. Yang, T. R. Jow, and P. N. Ross, *J. Phys. Chem. B*, **109**, 17567 (2005).
82. H. Zheng, L. Chai, X. Song, and V. Battaglia, *Electrochim. Acta*, **62**, 256 (2012).
83. P. M. Attia, W. C. Chueh, and S. J. Harris, *J. Electrochem. Soc.*, **167**, 090535 (2020).
84. L. von Kolzenberg, A. Latz, and B. Horstmann, *ChemSusChem*, **13**, 3901 (2020).
85. The MathWorks Inc., (2022), MATLAB version: 9.13.0 (R2022b), Natick, Massachusetts: The MathWorks Inc. <https://www.mathworks.com>.
86. S. A. Delp, O. Borodin, M. Olguin, C. G. Eisner, J. L. Allen, and T. R. Jow, *Electrochim. Acta*, **209**, 498 (2016).
87. T. Hou, G. Yang, N. N. Rajput, J. Self, S.-W. Park, J. Nanda, and K. A. Persson, *Nano Energy*, **64**, 103881 (2019).
88. F. Single, B. Horstmann, and A. Latz, *J. Electrochem. Soc.*, **164**, E3132 (2017).
89. P. Lu, C. Li, E. W. Schneider, and S. J. Harris, *The Journal of Physical Chemistry C*, **118**, 896 (2014).
90. O. Borodin, *Current Opinion in Electrochemistry*, **13**, 86 (2019).
91. Z. Li, Y. Chen, X. Yun, P. Gao, C. Zheng, and P. Xiao, *Adv. Funct. Mater.*, **33**, 2300502 (2023).
92. J. Chen, X. Fan, Q. Li, H. Yang, M. R. Khoshi, Y. Xu, S. Hwang, L. Chen, X. Ji, and C. Yang, *Nat. Energy*, **5**, 386 (2020).
93. A.-M. Li, Z. Wang, T. P. Pollard, W. Zhang, S. Tan, T. Li, C. Jayawardana, S.-C. Liou, J. Rao, and B. L. Lucht, *Nat. Commun.*, **15**, 1 (2024).
94. Y. Wang, Z. Wu, F. M. Azad, Y. Zhu, L. Wang, C. J. Hawker, A. K. Whittaker, M. Forsyth, and C. Zhang, *Nature Reviews Materials*, **9**, 119 (2024).
95. S. Jiao, X. Ren, R. Cao, M. H. Engelhard, Y. Liu, D. Hu, D. Mei, J. Zheng, W. Zhao, and Q. Li, *Nat. Energy*, **3**, 739 (2018).
96. K. Knehr, J. Kubal, and S. Ahmed, "Cost analysis and projections for US-Manufactured automotive lithium-ion batteries." *Argonne National Laboratory (ANL)* (Argonne National Lab., Argonne, IL (United States)) (2024), <https://www.osti.gov/biblio/2280913>.
97. M. D. Garayt, M. B. Johnson, L. Laidlaw, M. A. McArthur, S. Trussler, J. E. Harlow, J. Dahn, and C. Yang, *J. Electrochem. Soc.*, **170**, 080516 (2023).
98. P. M. Attia, A. Bills, F. B. Planella, P. Dechent, G. Dos Reis, M. Dubarry, P. Gasper, R. Gilchrist, S. Greenbank, and D. Howey, *J. Electrochem. Soc.*, **169**, 060517 (2022).
99. G. F. Pach et al., *J. Mater. Chem. A*, **9**, 2492 (2024).
100. J. Landesfeind and H. A. Gasteiger, *J. Electrochem. Soc.*, **166**, A3079 (2019).
101. M. Nie, D. P. Abraham, Y. Chen, A. Bose, and B. L. Lucht, *The Journal of Physical Chemistry C*, **117**, 13403 (2013).